Hydrol. Earth Syst. Sci. Discuss., 10, 4951–5011, 2013
www.hydrol-earth-syst-sci-discuss.net/10/4951/2013/
doi:10.5194/hessd-10-4951-2013

Hydrology and Earth System Sciences
Open Access
Discussions

Uncertainty analysis in model parameters regionalization: a case study involving the SWAT model in Mediterranean catchments (Southern France)

H. Sellami[1], I. La Jeunesse[2,3], S. Benabdallah[4], N. Baghdadi[5], and M. Vanclooster[1]

[1]Earth and Life Institute, Université catholique de Louvain, Croix du Sud 2, Box 2, 1348 Louvain-la-Neuve, Belgium
[2]CITERES, Université de Tours, UMR6173, 33 allée Ferdinand de Lesseps BP 60449 – 37204 Tours cedex 3, France
[3]LETG-Angers LEESA, UMR6554, CNRS, University of Angers, Faculty of Sciences 2 Bd Lavoisier, 49045 Angers Cedex 1, France
[4]Centre de Recherches et des Technologies des Eaux, Technopole Borj Cedria, BP 273, Soliman 8020, Tunisia
[5]IRSTEA, UMR TETIS, 500 rue François Breton, 34093 Montpellier cedex 5, France

Received: 4 February 2013 – Accepted: 8 April 2013 – Published: 18 April 2013

Correspondence to: H. Sellami (haysellami@yahoo.fr)

Published by Copernicus Publications on behalf of the European Geosciences Union.

Abstract

In this study a method for propagating the hydrological model uncertainty in discharge predictions of ungauged Mediterranean catchments using a model parameter regionalization approach is presented. The method is developed and tested for the Thau catchment located in southern France using the SWAT hydrological model. Regionalization of model parameters based on physical similarity measured between gauged and ungauged catchments attributes is a popular methodology for discharge prediction in ungauged basins, but it is often confronted with an arbitrary criterion for selecting the "behavioral" model parameters sets (Mps) at the gauged catchment. A more objective method is provided in this paper where the transferrable Mps are selected based on the similarity between the donor and the receptor catchments. In addition, the method allows propagating the modeling uncertainty while transferring the Mps to the ungauged catchments. Results indicate that physically similar catchments located within the same geographic and climatic region may exhibit similar hydrological behavior and can also be affected by similar model prediction uncertainty. Furthermore, the results suggest that model prediction uncertainty at the ungauged catchment increases as the dissimilarity between the donor and the receptor catchments increases. The methodology presented in this paper can be replicated and used in regionalization of any hydrological model parameters for estimating streamflow at ungauged catchment.

1 Introduction

Hydrological models are generally calibrated against observation variable(s), typically streamflow, to estimate some parameters that cannot be measured directly and to achieve a reliable prediction of the watershed response. However, in many cases, observed streamflow data are not available or are insufficient and, therefore, the catchment is considered as ungauged (Sivapalan et al., 2003) which may undermine the planning and the management of the water resources in the ungauged catchment. To

HESSD
10, 4951–5011, 2013

overcome this problem, various regionalization techniques have been developed to estimate streamflow in ungauged catchments including methods based on the similarity approach (Vandewiele and Elias, 1995; Idrissi et al., 1999; Merz and Blöschl, 2004; McIntyre et al., 2005; Oudin et al., 2008) and the statistical approach (Sivapalan et al., 2003; Yadav et al., 2007). The latter approach consists of deriving statistical relationships between catchment attributes (CAs), such as topography, soil, drainage area, etc., and the optimized model parameter (Mps). Once these relationships have been established, one can determine the parameters of an ungauged basin using its CAs. Although it can be considered as the most common regionalization approach for ungauged catchment (Wagener and Wheater, 2006), statistical approaches were deeply criticized due to the assumption that most statistical models consider linearity between CAs and optimized Mps. On the other hand, regionalization based on the similarity approach consists of transferring the information from donor catchment(s) to receptor catchment(s). It involves the following steps: (1) the identification of donor catchment(s), usually a gauged catchment(s), that is (are) most likely to be hydrologically similar to the receptor catchment(s) (ungauged catchment(s)), and (2) the transfer of the relevant information (Mps or streamflow records) from donor to receptor catchment(s). Typically, Mps transfer from donor to receptor catchment(s) rely on either physical similarity measures. In this case, the same CAs as used in the statistical technique can be adopted to identify similar catchments. Alternatively, use can be made of spatial proximity measures (e.g. the distance between the centroids of the catchments). The similarity regionalization approach is lying on the assumption that similar catchments behave hydrologically similarly. So, the definition of the similarity measure, certainly subjective, will condition the success of the selected regionalization approach (Heuvelmans et al., 2006).

Several studies have focused on the transfer of Mps based on similarity approach for predicting streamflow records at ungauged catchments (Merz and Blöschl, 2004; McIntyre et al., 2005; Parajka et al., 2005; Bàrdossy, 2007; Oudin, et al., 2008). For example, McIntyre et al. (2005) found that Mps transfer outperformed as compared to

HESSD
10, 4951–5011, 2013

the statistical regression approach using a five parameters version of the PDM model, applied on 127 UK catchments. Similar conclusions were drawn by Oudin et al. (2008) using two conceptual rainfall-runoff models, GR4J and TOPMO, in 913 French catchments. Parajka et al. (2005) showed also that similarity based regionalization approach outperformed as compared to the regression approach. But, they concluded that the best performing regionalization method was a kriging method based on nearest neighbor interpolation, followed by the similarity approach based on similarity of CAs between the donor and the receptor catchment. Other studies have reported that even nearby catchments can be hydrologically different (Beven, 2000).

The similarity approach for regionalization of Mps in ungauged catchments implies the "good" performance of the calibrated hydrological model at the donor catchment. Then, Mps that lead to "good" or "behavioral" model simulations are selected and transferred to the ungauged catchment. However, it is argued that hydrological model predictions, even in well gauged catchments are subject to inherent uncertainty that stems from different uncertainty sources (e.g. inputs, parameter uncertainty, model structure, and observed data). Because of all these uncertainty sources, it is expected and argued that model calibration will lead to non-unique sets of parameters (Beven and Binley, 1992) and, hence, it becomes difficult to associate the parameters estimated through calibration with the physical characteristics of the catchment. While model parameters uncertainty at well gauged catchment has received considerable attention during the past two decades (Beven and Binley, 1992; Duan et al., 1992; Abbaspour et al., 1997; Muleta and Nicklow, 2005; Vrugt et al., 2008; Yang et al., 2008; Zhang et al., 2009; Shen et al., 2012), a little attention has been given to the uncertainty resulting from Mps regionalization at the ungauged sites (Wagener and Wheater, 2006). Furthermore, additional uncertainty related to the regionalization procedure that stems from the arbitrary choices of the CAs, or the similarity measure, or the selection of the candidate parameter sets to be transferred can have a significant effect on the model prediction uncertainty in the ungauged catchments. Addressing all these sources of

HESSD
10, 4951–5011, 2013

uncertainty and understanding the way they can affect the model prediction in the ungauged catchment is a challenging task (Sivapalan et al., 2003; Wagener et al., 2004).

This paper aims to contribute to this challenge by addressing the following question: how can Mps uncertainty of donor catchments be propagated through regionalization schemes based on the similarity approach, and how does it affect the prediction uncertainty in ungauged catchment? Specific questions are: (1) is the selected hydrological model suitable for reproducing the hydrology in the ungauged catchment? (2) How does parameter uncertainty affect model prediction uncertainty in the ungauged catchment through the regionalization scheme?

In an attempt to answer to these research questions, the paper is organized in 3 main sections. In the first section the study site, the data available, the modeling approach and the regionalization procedure are described. The second section describes and discusses the results of the modeling and the regionalization approach. The final section reports the main outcomes of the paper as a summary and conclusions.

2 Study site description and available data

2.1 Study site description

The Thau catchment is located on the French Mediterranean coast (Languedoc-Rousillon region) and drains an area of approximately 280 km^2. The catchment is drained by ten streams that flow directly into the lagoon (Fig. 1). The basins size varies from 3.42 km^2 to 67 km^2 with the biggest one corresponding to the Vène catchment. Other geomorphologic and topographic characteristics of these catchments are given in Table 1. Dominant land use types within the study site are vineyards and non-agriculture vegetation (trees, Mediterranean sclerophyllous vegetation). The distribution of the main land use within each sub-catchment is given in Table 1. The eastern part of the Thau catchment area is composed of Jurassic limestone overlaid by Miocene marls in its central part, corresponding to 60 % of the Vène watershed surface. These Jurassic limestone are characterized by the presence of a large karstic aquifer whose limits extend the topographic limit of the catchment and strongly influences the hydrological regime of the Vène catchment (Plus et al., 2006; Gallart et al., 2008; Perrin and Tournoud, 2009; Chahinian et al., 2011). Soils in this part of the Thau catchment are mainly sandy-loam and silty-loam soils with porosity ranging from 35 to 50 % at 1 m depth of the soil profile. The western part of the Thau catchment is composed of the Eocene marls overlaid mainly by the Miocene marls. This region covers the central part of the Pallas, Aygues_Vacques, Nègues_Vacques, Mayroual, Soupié and Fontanilles catchments with silty-clayey-loam and loam textured soils so that runoff generation process are expected to be different from the eastern part.

2.2 Available data

The climate is a typical Mediterranean regime characterized by a large seasonal variability of rainfall in time and space with an annual average value of 600 mm. Precipitation occurs as short intense storms mainly during autumn and spring (from September to January) and separated by a long dry period (from February to August). The hottest months are July and August where the maximum temperature can exceed 35 °C and the coldest months are December and January where daily minimum temperature can reach −5 °C.

Data such as a Digital Elevation Model (50 m grid, provided by the French National Geographic Institute), a soil map (50 m resolution, provided by the INRA Montpellier) and land use maps (50 m resolution) for 1996 (La Jeunesse et al., 2002) and 2010 are available for each catchment. Daily precipitation data (from 1990 to 1999) are provided by five rain gauge stations located within the study area but only the Sète rain gage (French national meteorological station of Météo France) has daily precipitation data that covers the 2007–2009 period (Fig. 1). Daily temperature is provided from the meteorological station of Sète. Daily wind speed, air relative humidity and solar radiation are provided from the meteorological station of Fréjorgues airport located 20 km in the northeastern of the Thau catchment.

HESSD
10, 4951–5011, 2013

In the Thau basin about two years (1994–1996) streamflow records are available for the Vène and the Pallas catchments, while for the other rivers, streamflow records are either missing or either have missing values and are not long enough to allow direct model calibration. The available streamflow records are different in time and length between the catchments. For instance, the Pallas and the Vène catchments have daily streamflow records covering the 1994–1996 periods, with 208 and 667 observations, respectively, while the Soupié and Fontanilles catchments have streamflow of 500 daily records but covering the 2007–2009 period. Daily discharge at the Aygues_Vacques and Joncas catchments covers the same time period (2007–2009) but with very short time series length (80 days) whereas the Lauze, Nègues_Vacques and Mayroual catchments do not have any streamflow records. Such a case of poorly gauged catchments is very common in semi-arid and Mediterranean area and, when coupled with discontinuities in flow regime of ephemeral rivers, make the modeling of the discharge challenging. Despite that observed streamflow time series are available for some catchments but at different time periods (1994–1996 and 2007–2009), climate characteristics (mean daily/annual precipitation, mean, maximum and minimum daily temperature, etc.), between these two time periods are relatively similar. However, land use and land cover (LULC) types between the time periods have undergone a slight change according to the LULC map of 1996 and 2010. Figure 2 shows the change of LULC occurred in the Pallas and in the Vène catchments between 1996 and 2010. It shows that the surface that are for vineyards have decreased by an average of 13 % whereas non-agriculture vegetation has increased by an average of 7 %. Despite that, it is well argued that LULC is one of the major drivers of the hydrological processes and catchment runoff response (Nathan and McMahon, 1990; Wagener et al., 2007). The study of the effect of land use change on model parameters regionalization approach results is, however, not within the objectives of this paper.

As the Pallas and the Vène catchments were subject to previous studies (La Jeunesse et al., 2002; Plus et al., 2006; Chahinian et al., 2011; Sellami et al., 2013) more detailed data are available for these subcatchments. Therefore, the Vène and the Pallas catchments are considered as gauged catchments, while all the other small catchments are considered ungauged.

3 Description of the hydrological model

The Soil and Water Assessment Tool (SWAT) (Arnold et al., 1998) is a continuous-time and physically based hydrological model. SWAT is developed to predict the impact of land management practices on water, sediment and agricultural chemical yields in large complex catchments with different soil, land use and management conditions over long periods of time (Eckhardt et al., 2005). The hydrological model operates by dividing the watershed into subbasins. Each subbasin is further discretized into a series of hydrologic response units (HRUs), which are unique soil-land use combinations. Soil water content, surface runoff, nutrient cycles, sediment yield, crop growth and management practices are simulated for each HRU and then aggregated for the subbasin by a weighted average. The hydrological balance is calculated based on the following equation:

$$\mathrm{SW}_t = \mathrm{SW}_0 + \sum_{i=1}^{t} \left(P - Q_{\mathrm{surf}} - E - W - Q_{\mathrm{gw}}\right)_i \tag{1}$$

where t is the time in days, SW_t is the final soil water content, SW_t is the initial soil water content, P is the precipitation on day (i), Q_{surf} is the surface runoff on day (i), E is the evapotranspiration on day (i), W is the amount of water percolated from the soil profile on day (i) and Q_{gw} is the return flow or groundwater flow that contributes to the streamflow on day (i). All parameters are expressed in (mm) over the catchment area.

The water in each HRU in SWAT is stored in four storage volumes: snow, soil profile, shallow aquifer, and deep aquifer. Surface runoff from daily rainfall is estimated using a modified SCS curve number method, which estimates the amount of runoff based on local land use, soil type, and antecedent moisture condition. Calculated flow, sediment yield, and nutrient loading obtained for each subbasin are then routed through the river channel using the variable storage or Muskingum method. The watershed concentration time is estimated using Manning's formula, considering both overland and channel flow.

The soil profile is subdivided into multiple layers that support soil water processes including infiltration, evaporation, plant uptake, lateral flow, and percolation to lower layers. The soil percolation component of SWAT uses a water storage capacity technique to predict flow through each soil layer in the root zone. Downward flow occurs when field capacity of a soil layer is exceeded and the layer below is not saturated. Percolation from the bottom of the soil profile recharges the shallow aquifer. The amount of water entering the shallow aquifer is a function of the total water volume exiting the soil profile and an exponential decay function to account for the recharge time delay (GW_DELAY). The latter is depending on the overlying geologic formations. If the depth of the shallow aquifer increases above the user defined threshold value (GWQMN), it is assumed that groundwater discharge is occurring and contributing to the reach. Upward flow movement to the overlaying unsaturated soil layers is simulated by routing water in the shallow aquifer storage component to the soil by capillary pressure or by direct absorption by the plant roots. This remove water process is termed "revap". The amount of water removed via "revap" is correlated to the parameter GW_REVAP.

The model computes evaporation from soils and plants separately. Potential evapotranspiration can be modelled with three options available in SWAT, that is, Penman-Monteith, Priestley–Taylor and Hargreaves methods (Neitsch et al., 2005), depending on data availability. Potential soil water evaporation is estimated as a function of potential ET and leaf area index. Actual soil evaporation is estimated by using exponential functions of soil depth and water content. Plant water evaporation is simulated as a linear function of potential ET, leaf area index, and root depth, and can be limited by soil water content. More detailed descriptions of the SWAT model can be found in Neitsch et al. (2005).

HESSD
10, 4951–5011, 2013

The SWAT simulations are conducted on the gauged catchments from 1990 to 1996 with 4 yr (1990–1993) as a warming-up period to minimize the effects of the initial state of SWAT variables on river flow. The modified SCS curve number method is chosen for surface runoff volume computing. The variable storage coefficient method is selected for the flow routing through the channel and potential evapotranspiration is estimated by the Penman-Monteith method. The daily stream flow data from 2 August 1994 to 1 September 1996 and from 25 November 1995 to 14 June 1996 for the Vène and the Pallas catchments, respectively, are used to assess the model prediction performances.

4 Modeling approach

4.1 Sensitivity analysis (SA)

A way to deal with high-dimensional hydrological models, such as SWAT, is to conduct SA to select only the sensitive model parameters that are assumed to represent the real system behavior. In the current study case, a SA is conducted using the built-in SWAT SA tool that uses the Latin Hypercube One-factor-AT-a Time (LH-OAT) (van Griensven et al., 2006) method. In the LH-OAT technique only one input parameter is modified between two successive model runs. Therefore, the change in model output can then be attributed to such parameter modification. Parameter that induces the highest model output change is ranked first and the less sensitive parameter is given a rank equals to the total number of parameters. A complete detailed explanation of this SA technique can be found in van Griensven et al. (2006).

SA is performed on 17 SWAT model parameters that may have a potential to influence the flow river. Snow parameters are not included in the SA since the study site belongs to a semi-arid climate and the flow is not affected by the snow melt process. The ranges of parameters variation are based on the SWAT manual (Neitsch et al., 2005) and are sampled by considering a uniform distribution (Yang et al., 2008;

HESSD
10, 4951–5011, 2013

Chahinian et al., 2011) in their physical range. Ten sensitive SWAT parameters are identified for each of the Pallas and the Vène catchment (Table 2). The identified sensitive parameters are the same for both cases but they differ in their rank. The first two ranked parameters are groundwater related parameters: ALPHA_BF (a parameter that expresses the recession or the rate at which the groundwater is returned to the flow) and GWQMN (a threshold depth of water in the shallow aquifer required to return flow). The third ranked parameter for the Vène river is GW_DELAY, which is defined as the required time for water leaving the bottom of the root zone to reach the shallow aquifer where it can contribute to lateral groundwater flow. This groundwater parameter is ranked 7th for the Pallas river. The third ranked parameter for the Pallas river is CN2, which is the initial SCS runoff curve number for moisture condition and that determines the volume of surface runoff contributing to the total stream flow. This latter parameter is a surface runoff parameter that depends on several factors including soil types, soil textures, soil permeability, land use properties, etc. The remaining sensitive parameters for the Vène and the Pallas catchments are mainly direct or indirect surface runoff parameters: CH_K, which is the hydraulic conductivity of the channel; CH_N, which is the manning's value of the tributary channel; ESCO, which is the soil evaporation compensation factor which directly influences the evapotranspiration losses from the watershed; EPCO, which is the plant uptake compensation factor and expresses the amount of water needed to meet the plant uptake demand; GW_REVAP, which is dimensionless coefficient controlling the rate of water movement between the root zone and the shallow aquifer; and SURLAG, which controls the fraction of the total water that is allowed to enter the stream on any specific day.

It is argued that in order to provide better identified models and to ensure high regionalization potential, the structure of the selected hydrological model should be reduced to only components that describe the key process of the system. Therefore, it is suggested that the number of required model parameter should not be more than half a dozen (Wagener et al., 2001). However, the approach to retain only the necessary model structure components (parsimonious model) do not necessary guarantees that

HESSD
10, 4951–5011, 2013

all the hydrological processes of the watershed are identified and represented, especially in complex hydrological systems. However, from the results of the SA and the physical meaning of the selected sensitive parameters it is obviously difficult to select less than 10 parameters in the current study cases. In addition, it is well known that the hydrological processes are complex in the study area due to the presence of the karstic aquifer in the Vène watershed (Plus et al., 2006; Gallart et al., 2008; Perrin and Tournoud, 2009; Chahinian et al., 2011). Hence, selecting the 10 sensitive parameters described above ensures that the model does not omit one or more hydrological processes important for this particular case study. Furthermore, other studies dealing with the SWAT model have identified more or less 10 sensitive parameters that are assumed to describe appropriately the hydrological process of the real system. For example, Heuvelmans et al. (2004) have identified 7 sensitive SWAT model parameters related to flow generation to be regionalized in Northern Belgium. Gitau and Chaubey (2010) have selected 16 SWAT parameters for flow prediction in ungauged catchments. Chahinian et al. (2011) have calibrated 14 SWAT model parameters for modeling flow and nutrient emission processes. They found that 12 sensitive parameters are directly and indirectly related to flow simulation.

4.2 Uncertainty analysis (UA)

The Generalized Likelihood Uncertainty Estimation, GLUE, (Beven and Binley, 1992) is selected for assessing the model parameter uncertainty. The reasons behind selecting GLUE are its simple concept, its relative ease of implementation and use without major modifications to the method itself. GLUE is a Monte Carlo based method for modelling uncertainty analysis (Beven and Binley, 1992; Freer et al., 1996, for details). GLUE is based on a large number of model runs with different combinations of the parameter values chosen randomly and independently from the prior distribution of the parameter space. By comparing predicted and observed responses, each set of parameter values is assigned a likelihood value (function that quantifies how well that particular parameter combination simulates the observed system); higher values of the likelihood

HESSD
10, 4951–5011, 2013

function typically indicate better correspondence between the model predictions and observations. Based on a cutoff threshold, the total sample of simulations is then split into "behavioral" and "non-behavioral" parameter combinations. The distribution of the likelihood value for "behavioral" sets is treated as a probabilistic weighting function for the predicted variables (Beven and Binley, 1992). According to this, a cumulative distribution of the model predictions is formulated and the desired quantiles are computed to represent the uncertainty. Uncertainty of a model is stated by giving a range (or a band) of values that are likely to enclose the true value of a specific simulated variable: stricter uncertainty bands demonstrate lower uncertainty while larger bands are caused by highly uncertain models. Using the concept of uncertainty, the "behavioral" models are these able to "correctly" simulate the variable of interest while minimizing the width of the uncertainty bands.

Some subjective choices are considered within the implementation of the GLUE framework in this study. The prior distributions of the selected parameters are assumed to follow a uniform distribution over their respective range (Table 2). This initial distribution is chosen since the real distribution of the parameter is unknown. Parameters ranges are chosen based on the SWAT manual (Neitsch et al., 2005) and previous GLUE applications with the SWAT model (Yang et al., 2008; Shen et al., 2012). To sample the prior parameter distribution in the GLUE methodology, a simple random sampling is implemented. The number of sampling sets is set to 10 000. Previous applications of GLUE with the SWAT model have used this number of model runs to assess uncertainty of about 10 sensitive SWAT model parameters (Yang et al., 2008; Gong et al., 2011). Moreover, it was mentioned by Yang et al. (2008) that no significant change was observed in the GLUE results between 10 000 and 20 000 model runs. So, the selected number of 10 000 simulations is considered reasonably sufficient for this study. The likelihood function selected is the Nash and Sutcliffe (1970) efficiency coefficient (NS) since it is widely used as a likelihood measure within GLUE in the literature (Beven and Freer, 2001; Arabi et al., 2007; Shen et al., 2012).

HESSD
10, 4951–5011, 2013

$$NS = 1 - \frac{\sum_{i=1}^{n} (P_i - O_i)^2}{\sum_{i=1}^{n} (O_i - \bar{O})^2} \quad (2)$$

with O_i is the observed value, $\bar{O}$ mean observed values and P_i is the predicted value. The range of NS lies between 1 (perfect fit) and $-\infty$.

The cutoff threshold selected to separate "behavioral" from "non-behavioral" parameter sets is another subjective choice within the GLUE method. Frequently, when the likelihood value is greater than zero the corresponding simulations are considered "behavioral" (Freni et al., 2010; Gong et al., 2011). For application of the GLUE method in this study, model simulations with negative NS values are considered unacceptable and, therefore, the corresponding parameter sets are discarded from further analysis.

The selection of the threshold value is an entirely arbitrary choice that affects the prediction uncertainty (Montanari, 2005; Mantovan and Todini, 2006) and probably is the most important concern for the GLUE method. A small cutoff threshold will lead to larger "behavioral" simulations and larger uncertainty bands, while larger threshold value will decrease the numbers of "behavioral" models and will reduce the uncertainly interval width (Xiong and O'Connor, 2008; Blasone et al., 2008; Viola et al., 2009). In addition, selecting a very high threshold value, to ensure that "behavioral" parameter set represent well the real system, may lead to identify only one parameter set as "optimal" which is inconsistent with the overall GLUE philosophy.

The selection of the confidence level has an impact on the parameter uncertainty analysis within the GLUE framework (Blasone et al., 2008; Jin et al., 2010; Gong et al., 2011). However, it is common that the 95 % confidence interval is used for the uncertainty analysis, despite that it may not be able to capture the entire observation variable and, hence, not representing all the uncertainty (Montanari, 2005; Beven, 2006; Xiong and O'Connor, 2008). As the GLUE method is dependent on all these subjective decisions that influence the final uncertainty prediction, it has been deeply criticized

HESSD
10, 4951–5011, 2013

and its several drawbacks have been well pointed out and discussed in the literature (Montanari, 2005; Mantovan and Todini, 2006).

4.3 The regionalization schemes

The adopted regionalization method for this study is the transfer of Mps from donor to receptor catchment based on the similarity between their physical attributes (topography, geology, soils, drainage area, etc.). The physical similarity approach is based on the assumption that catchment physiographic characteristics predetermine the hydrological behavior. Therefore, a selection of relevant CAs is crucial for the success of the regionalization procedure. The catchments attributes (CAs) selected and used to define similarity are related to topography, land cover, drainage area, soil and geology features (Table 1). They are derived from the available data such as land use maps, soil maps, digital elevation model and geology maps. These CAs are generally considered as the main drivers of the hydrological process in the literature and are the most common ones used to define similarity between catchments in model parameter regionalization schemes (Merz and Blöschl, 2004; Heuvelmans et al., 2006; Wagener et al., 2007; Bastola et al., 2008). For instance, Heuvelmans et al. (2006) have considered catchment area, average slope, dominant land use and soil texture classes as the most appropriate catchment descriptors in model parameters regionalization in Flemish part of the Scheldt river basin (Belgium). Besides these CAs, others authors have used flow indices or characteristics using FDC (Masih et al., 2010), indices of hydrological responses (Yadav et al., 2007) or hydro-meteorological long term data (Bastola et al., 2008) as relevant catchment descriptors. However, the selection of the appropriate CAs depends also on the physical meaning of the selected model parameters, on the objective of the regionalization procedure and on the knowledge about the key hydrological processes accruing within the catchment. For example, when the objective of the regionalization procedure is to estimate the flow in ungauged catchments, as in our case, the use of flow characteristics or indices as input is useless. Model parameters, especially theses of physically based model such as SWAT, are assumed

HESSD
10, 4951–5011, 2013

to be closely related to CAs and, thus, represent the functional beahviour of the catchment response. For instance, in the SWAT model the curve number parameter (CN2) depends on the soil and land use characteristics of the catchment, therefore, they are considered among the relevant catchment descriptors. Knowledge about the key process in the system can also assist the selection of the relevant CAs. As an example, the geology is considered as relevant catchment descriptor in our study case since it is known that the Jurassic limestone aquifer in the eastern part of the Thau catchment strongly influences the hydrological regime of the Vène catchment (Sellami et al., 2013).

The soil characteristics are based on the dominant soil texture (% clay, % silt, % sand) within each catchment. The main geological feature considered is the surface catchment percentage covered by the Jurassic limestone estimated using the GIS tools based on a simplified geological map of the Thau catchment. Other geomorphologic and topographic descriptors (mean elevation, mean slope, drainage area) are also calculated using GIS tools and are reported in Table 1. Besides the CAs, it is very common that climatic characteristics such as long-term precipitation characteristics, the annual precipitation, annual potential evapotranspiration index, solar radiation, etc. (see, Wagener et al., 2007), are used for the similarity measure between the catchments. However, in our case study such climatic descriptors are omitted since we are dealing with small and geographically close catchments located within a relatively small area under the same climate regime.

Unfortunately, there does not exist a universally accepted metric or combination of metrics to quantify catchments similarity in the catchment attribute space. Some authors have used the inverse of the Euclidean distance (Heuvelmans et al., 2004) in the catchment attribute space. Others (Parajka et al., 2005) have used the normalized sum of the absolute difference between catchment attributes, while, again, others authors (Masih et al., 2010) have used the weighted normalized sum of the absolute difference where the user can assign equal or more weight to individual catchments attributes in order to consider their varying assumed importance. To identify similar catchments

HESSD
10, 4951–5011, 2013

Uncertainty analysis in model parameters regionalization

H. Sellami et al.

groups, catchments can be merged into a larger cluster in a hierarchical way. At each step the average link distance between clusters using the average linkage method can be computed and the clusters with the largest similarity are merged. The Pearson's correlation coefficient, denote hereafter as R^2, can be used as a similarity metric between catchment attributes; the higher the R^2 between the target and the donor catchments, the more similar they are. Once the clusters are established, information can be transposed from donor(s) to receptor(s) catchment(s). In complex hydrological models this transfer of information is a difficult task due to the parameter uncertainty, to their interdependency, to the non-unique solution and to other various sources of uncertainty (Bárdossy, 2007). Some authors, Heuvelmans et al. (2004); McIntyre et al. (2005); Bárdossy (2007); Oudin et al. (2008) and He et al. (2011), suggest the transfer of the entire parameter sets to the ungauged catchment(s) justifying that transferring the entire parameter sets does not interfere with the integrity of the model parameters as a set and that the entire hydrological processes are considered at once.

The traditional way of transferring the Mps from donor(s) to receptor(s) catchment(s) can also be based on the selection of the "behavioral" Mps obtained from simulations with likelihood values (e.g. NS coefficient) above certain user defined threshold value at the donor(s) catchment(s). However, doing this way all the receptor(s) catchment(s) will receive equal number of Mps despite that they are not equally similar to the donor(s) catchment(s). This may overestimate the prediction uncertainty at the closest receptor(s) catchment(s) and may underestimate it at catchments that are further from the donor(s) catchment(s). Furthermore, the selection of the "behavioral" Mps is based on an arbitrary and entirely subjective choice of a threshold value which may add to the uncertainty of the final regionalization results.

In this section we propose a more objective method for selecting the appropriate Mps sets to be transferred from gauged catchment(s) to ungauged catchment(s). The method is based on the similarity metric and consists in (i) retaining the GLUE Mps that led to positive simulations (NS > 0) in the gauged catchment(s), (ii) using the similarity measure value between the donor(s) and the receptor(s) catchment(s) as a threshold

HESSD
10, 4951–5011, 2013

value to determine the candidate parameter sets and (iii) transferring the selected entire unchanged parameter sets to the ungauged catchment(s) and calculating the corresponding prediction uncertainty interval. The threshold metric used in this approach is defined as follows:

$$\mathrm{Thresh}_{(\mathrm{d,r})} = R^2_{(\mathrm{d,r})} \times \max \mathrm{NS_d} \tag{3}$$

where $R^2_{(\mathrm{d,r})}$ is the similarity measure between the donor catchment (d) and the receptor catchment (r) and scaled between 0 and 1 and $\mathrm{NS_d}$ is the highest likelihood value reached in the model simulations at the donor catchment (d). To compute the threshold value ($\mathrm{Thresh}_{(\mathrm{d,r})}$), the similarity matrix between all catchments attributes is calculated (data not shown). By applying Eq. (3) the number of the candidate Mps will increase linearly as the dissimilarity between the donor(s) and the receptor(s) catchment(s) increases. Furthermore, besides parameter uncertainty, additional uncertainty related to the regionalization schemes is explicitly accounted in the final model prediction uncertainty at the ungauged catchment(s) by introducing the similarity measure in Eq. (3). As the dissimilarity between the donor(s) and the target catchment(s) increases, model prediction uncertainty in the target catchment(s) intuitively increases and vice versa. Another advantage of using Eq. (3) is that the selection of the threshold value to define the number of the candidate Mps is based on the similarity metric rather than on a subjective choice of the modeler which may reduce this additional uncertainty component in the final regionalization procedure. Once the threshold value (Thresh) is calculated the entire selected Mps is transferred from the donor catchment(s) to the receptor(s) catchment(s).

To transfer the entire parameter sets derived by GLUE in the gauged catchment(s) without further change and update the parameter values in its corresponding SWAT text file, a sampling and rewriting program in the MATLAB® computing language was developed and linked to the GLUE and the SWAT model.

HESSD
10, 4951–5011, 2013

4.4 Modeling evaluation criteria

Besides the NS statistical criteria the correlation coefficient R^2 is used to assess the goodness of fit between observation and the SWAT model simulations. The SWAT Model prediction uncertainty is quantified by the p factor which is the percentage of measured data bracketed by the 95 % prediction uncertainty (95 PPU) and by a measure of the Average Relative Interval Length (ARIL) proposed by Jin et al. (2010). However, for a more efficient comparison between the ungauged catchments without observations data, the ARIL was modified by standardizing the upper and lower boundary values of the simulated point by its mean value. The modified ARIL is called, hereafter, the Average Standardized Relative Interval Length (ASRIL).

$$p \text{ factor} = \frac{NQ_{\text{in}}}{n} \times 100 \quad (4)$$

$$\text{ASRIL} = \frac{1}{m}\sum_{t=1}^{m}\frac{Q^M_{t,97.5\,\%} - Q^M_{t,2.5\,\%}}{\text{Mean}(Q^M_t)} \quad (5)$$

where NQ_{in} is the number of observed discharge falling in the 95 PPU, $Q^M_{t,97.5\,\%}$ and $Q^M_{t,2.5\,\%}$ represent the upper and lower simulated boundary, respectively, at time t of the 95 PPU, n is the number of observation data points, m is the length of simulation, the subscript M refers to simulated, t refers to the simulation time step. The goodness of calibration and prediction uncertainty was judged on the basis of the closeness of the p factor to 100 % (i.e., all observations are bracketed by the 95 PPU) and the ASRIL to 0 (if there is no uncertainty, the value of ASRIL is zero). A small value of ASRIL and higher value of p factor represent better performance.

To assess the relative performances of the regionalization procedure for flow estimation in ungauged catchments, usually the simulated flow is compared to the observed one and/or sometimes gauged catchments are considered in turn as if they

HESSD
10, 4951–5011, 2013

are ungauged (Oudin et al., 2008). In the current work, catchments have very scarce streamflow records. Therefore any available observation data, field knowledge and/or previous work conducted in the area of interest can be precious and helpful to check the performance of the adopted regionalization method. Performance assessment of the regionalization procedure is based on three evaluation criteria. The first one namely fit to observation (van Griensven et al., 2012) and consists of the quantitative assessment of model accuracy simulations compared to measurements using some statistical criteria. In this regard, the simulated FDCs flow percentiles are compared to the observed ones by using the NS coefficient and the model prediction uncertainty is assessed through the *p* factor (percentage of observed data bracketed in the 95 % uncertainty interval) wherever observation data are available. The second one is called fit to reality (van Griensven et al., 2012) and consists of the evaluation of the model capability in reproducing the real hydrological process and in reflecting the reality of the field. For instance, the predicted mass balance can be calculated and used to assess the performance of the regionalization procedure in representing the main hydrological process that govern the hydrology of the study region. The third evaluation criterion is called fit to geography and it consists of mapping the predicted variable in order to check the soundness of its spatial distribution with some observed data (e.g. soil moisture map) or with some field knowledge (e.g. geology, karstic system, etc.).

5 Results and discussions

5.1 Model performances and prediction uncertainty at the gauged catchments

The NS values range from 0 to 0.71 with an average value of 0.47 for the Vène catchment while they range from 0 to 0.76 with an average value of 0.60 for the Pallas catchment. The correlation coefficient (R^2) is higher than 0.80 in both catchments indicating that SWAT is able to satisfactorily reproduce the general behavior of the observed hydrograph of both watersheds. The GLUE parameter sets are more robust and consistent in providing simulations that match better the observations of the Pallas catchment than these of the Vène catchment.

The 95 % GLUE prediction interval (95 PPU) is considered for uncertainty analysis. The average width of the 95 PPU is evaluated using the ASRIL and the percentage of data bracketed by this interval is estimated using the p factor. The 95 % GLUE uncertainty interval for the Vène and the Pallas catchments is plotted in Fig. 3. The ASRIL and the p factor are 2.48 and 70 % for the Pallas catchment, while the same statistics are 2.75 and 63 % for the Vène catchment, respectively. The ASRIL values indicate larger uncertainty interval in the Vène catchment than in the Pallas catchment. The statistics are far from their suggested values (ASRIL $\approx$ 0 and p factor $\approx$ 100 %) which indicate wide uncertainty prediction. Theoretically, by selecting the 95 % prediction interval one would expect a p factor of 95 %. However, this is not the case in the current GLUE results. The p factor in both watersheds is lower than the specified prediction level. This suggests that parameter uncertainty alone cannot compensate for all modeling uncertainty sources (e.g. input data, parameter uncertainty, model structure uncertainty, error in the measured data, etc.). In addition, this difference can also be due the subjectivity involved within the GLUE procedure for selecting the threshold value, the likelihood function, the initial parameter distribution, etc. This result is consistent with those reported in the literature (Xiong and O'Connor, 2008; Shrestha et al., 2009).

It is clear from the statistical factors and the graphical inspection of Fig. 3, that even though the 95 PPU of the Vène catchment is larger than the Pallas one, the former is bracketing more observation data. In addition, the predicted recession flow and baseflow are both affected with wide uncertainty, especially these of the Vène catchment. The difference in the 95 PPU interval width between the two catchments can be explained by the influence of the karstic system. Indeed, it was shown in previous studies (Gallart et al., 2008; Perrin and Tournoud, 2009; Chahinian et al., 2011) that the Vène streamflow is considerably dependent on the karst contribution. The Karst term is generally used to refer to subterranean area where groundwater flows in conduits and channel and can contribute to the surface stream through springs. The karst features

HESSD
10, 4951–5011, 2013

in the Vène catchment derive from the dissolution of the Jurassic limestone in the Thau catchment (Aquilina et al., 2002). However, these karst features are difficult, even impossible, to be accurately represented within the current SWAT framework. Indeed, the knowledge limitations concern the precise localization within the Vène catchment of the karst features such as springs, sinkholes and the real extend of the whole karstic network and their characteristics (drainage area, hydraulic conductivity, groundwater conduits network, etc.). Model structure limitations are due to the inaccurate representation of the real hydrogeological boundaries of the Vène karst system, which exceeds its topographic boundaries. Therefore, much less water is simulated by the model than the real water that may contribute to the Vène streamflow. In addition, in the SWAT model, water that infiltrates through the soil recharges the aquifer and contributes to the return flow within the same subbasin. Transfer of water from one subbasin to another is not allowed. However, springs can receive water from an extended karstic network that exceeds the topographic boundaries of the subcatchment. Other studies (Spruill et al., 2000; Coffey et al., 2004; Benham et al., 2006) have reported the difficulty of the SWAT model to accurately represent karstic-fed catchment. Afinowicz et al. (2005) have concluded that SWAT needs major change to adequately simulate baseflow and return flow. Such SWAT modification was adopted by Baffaut and Benson (2009) to allow faster percolation through the soil substrate and recharge of the aquifer to simulate quick movement of water through vertical conduits that characterize karst topography. Their results showed improved partitioning of streamflow between surface and return flow and significant sustainable flow, even during summers with lack of precipitation. However, the conceptualization of the karst system and the SWAT code change are beyond the scope of this study.

Besides the model prediction uncertainty, the parameters correlation and posterior distribution are investigated (results not shown). It is noted that different GLUE parameter combinations lead to similar model results in both case study. This is known as the equifinality concept (Beven and Binley, 1992) which is behind the GLUE method philosophy. Equifinality originates from the imperfect knowledge of the system under

HESSD
10, 4951–5011, 2013

consideration and from different error sources (errors in input and boundaries conditions, errors in using an approximate model structure of the real system and error in the observation variable being modelled) that can interact in a non-linear way (Beven, 2006). In addition, some parameters depicted as very sensitive by the SA method turned out to be less sensitive or less important by the GLUE method, such as ALPHA_BF and GWQMN. In fact, given the equifinality behind the GLUE concept and the possible correlations and interactions between parameters, a single parameter may lose in importance in the context of a combination of parameters values. As a corollary, GLUE cannot reveal the sensitivity of a single parameter.

The posterior parameters distribution (PDs) derived from the Monte Carlo runs are large and rather uniformly distributed over their range. This is because GLUE tends to flatten the response surface of the parameter by given equally weight to behavioral model runs. These results are consistent with previous studies (e.g. Yang et al., 2008; Dotto et al., 2012). However, the PDs shape and the uncertainty range of the parameters is dependent on the selected threshold value (Fig. 4). By selecting a threshold $NS \geq 0$, all parameters are rather uniformly distributed which lead to non-identifiable parameters indicating wide parameter uncertainty. While increasing the threshold value to $NS = 0.60$, some parameter PDs become narrower and peakier and well identified. This is illustrated in Fig. 4 for the example of the CN2 and GW_DELAY for the Vène catchment, and CN2 and SURLAG parameters for the Pallas catchment. In addition to the shape of the parameter PDs, increasing the threshold value results in a decline of the numbers of "behavioral" Mps retained and causes the depletion of the coverage of the observation by the GLUE uncertainty interval. For instance, by selecting a threshold value $NS \geq 0.60$, the p factor decreased from 70 % to 46 % and from 63 % to 53 % for the Pallas and the Vène catchments, respectively. The ASRIL also decreased to 2.23 and to 1.92 in the Vène and in the Pallas catchments, respectively, following the increase of the threshold value. These results are in accordance with the findings of Blasone et al. (2008) and Gong et al. (2011) and suggest that interpretation of parameter uncertainty derived by GLUE is always conditioned to the choices of threshold value and the prediction uncertainty level.

Investigations of the parameters correlation matrices (data not shown) show very low correlation between the parameters. It seems that GLUE does not explicitly account for parameters interaction. Many authors (Blasone et al., 2008; Yang et al., 2008; Jin et al., 2010) have reported the weak correlation between parameters within the GLUE method. One explanation can be that the selected sampling strategy cannot account for parameters interaction since each parameter is individually randomly sampled from its distribution.

5.2 Results of the regionalization approach

5.2.1 Catchments clustering

The similarity metric based on the multidimensional space of CAs resulted into 4 ungauged catchments similar to the Vène catchment (Lauze, Aiguilles, Joncas and Mayroual) and 4 ungauged catchments similar to the Pallas catchment (Fontanilles, Aiguilles, Nègues_Vacques and Soupié). Catchments within the same group are assumed to have similar hydrological behavior. The catchments clusters and the numbers of the candidate Mps transferred from the donor to the receptor(s) catchment(s), calculated using the similarity measure, are given in Table 3. The Vène and the Pallas catchment are identified as the donor catchments while all the others ungauged watersheds are considered as receptor catchments. The highest threshold value (Thresh) calculated using Eq. (3) is Thresh = 0.50 and 0.66 for the Vène and the Pallas catchment, respectively. These Thresh values are frequently used in literature to identify "behavioral" Mps (Gassman et al., 2007; Shen et al., 2012). The lowest Thresh values range between 0.25 and 0.38 corresponding to a transfer of 89.18 % and of 96.52 % of the total Mps sets of the Vène and the Pallas catchments, respectively (Table 3). These Thresh values correspond to poor model performances at the gauged catchments and can be seen as low compared to what has been usually used in literature. However, as it

HESSD
10, 4951–5011, 2013

was reported by Oudin et al. (2008), it is not straightforward to state whether or not poorly modeled gauged catchment(s) parameters should be transferred to ungauged catchment(s). From one side, it is expected that Mps associated with poorly modeled hydrographs in gauged catchment(s) will yield poor model performances at the ungauged catchment(s). On the other side, transfer of Mps of poorly modeled gauged catchment(s) may add a diversity which can be beneficial for modeling the ungauged catchment (Oudin et al., 2008).

5.2.2 Predicted Flow Duration Curves (FDCs) at the ungauged catchments

The FDC provides the percentage of time (duration) a daily or monthly (or some other time interval) streamflow is exceeded over a period for a particular river basin (Castellarin et al., 2004). FDC may also be viewed as the complement of the cumulative distribution function of the considered streamflow and is probably one of the most informative methods of displaying the complete range of river discharges, from low flows to flood events. Empirical FDCs can be easily constructed from streamflow observations using standardized non-parametric procedures (see Vogel and Fennessey, 1994, 1995; Smakhtin, 2001; Castellarin et al., 2004). The FDC concerns only the flow magnitude whereas the streamflow time series concerns both magnitude and time sequence. The flow percentiles conceptually represent different segments of the FDC: high flow ($\leq$ Q10), median flows (Q10–Q50) and low flows (Q50–Q100). The simulated FDCs resulting from the transfer of the GLUE Mps sets of the Pallas and the Vène catchment to the ungauged catchments, within their corresponding group, are plotted in Fig. 5.

The slope of the simulated FDCs within the high flow percentiles ($\leq$ Q10) is relatively steep for the two catchments groups, indicating that flood discharges are not sustained for a long period of time. The slope of the end tail of the simulated FDCs, corresponding to low flow ($\geq$ Q50), is steeper in the Pallas catchment group, while it is flattened out considerably in the Vène catchments group. This reflects the difference in the low flow regime between the two catchments groups. Catchments of the

HESSD
10, 4951–5011, 2013

Pallas group cease flowing at 20 % to 40 % of the simulation time period, while catchments of the Vène group have more sustained baseflow contribution. Figure 6 shows the coefficient of variation (CV = Standard deviation/Mean) and the mean magnitude of the simulated FDCs flow percentiles for all the catchments and quantify their inter and intra-catchments groups variability. It is clearly seen from Fig. 6 that the CV of the mean for all the FDCs flow percentiles within the Pallas catchments group is higher at low flows than at higher flows while, for the Vène catchments group, the CV is more or less steady across the flow percentiles, except for the Mayroual catchment. The intra-catchments variability of the CV of the flow percentiles within each catchment group shows that catchments within each group converge to a similar low flow CV value, except for the FDCs of the Fontanilles within the Pallas group and the Mayroual within the Vène group. It is worth noting here, that these catchments exhibit the largest dissimilarity in their physical attributes form their corresponding donor catchments. It is also clear in Fig. 6 that the simulated mean flow magnitude of the different flow percentiles is very low in both catchments group. The mean values of the high flow percentiles in both catchments group do not exceed 0.015 $m^3 s^{-1}$. However, the variation in the mean values of the simulated FDCs is more important in high flow percentiles than in low flow percentiles in both catchment groups. In the Pallas catchment group, the mean flow magnitude decreases rapidly from Q10 to Q20, then progressively from Q20 to Q50 leading to progressive increase in the CV within these flow percentiles and tends to be steady for flow percentile higher than Q50, which results in higher CV values. In addition, at low flow percentiles (> Q50), all the simulated FDCs of the Pallas catchment group tend to have similar mean flow values which resulted in less variability of the CV at the low flow percentiles. Also, catchments within the Vène group have much more variability in their simulated flow percentiles mean values than these of the Pallas group. The flow percentiles of the simulated FDCs of the Aiguilles catchment have the highest mean values while the Mayroual and Lauze FDCs flow percentiles are very similar and these of the Joncas catchment are the lowest values. It is worth noting here to add that the CV of low flow percentiles is also compared to the catchments

HESSD
10, 4951–5011, 2013

drainage area and to the soil characteristics within each ungauged catchment, but no clear relationships is found.

5.2.3 Uncertainty in the predicted FDCs at the ungauged catchments

The uncertain simulated FDCs are represented in Fig. 5 in such a way that dissimilarity between the donor and the receptor catchment, within each catchments group, increases from the left to the right and from top to down. It is clearly seen form Fig. 5 that the FDCs uncertainty interval in both catchments groups is wider as the receptor catchment is further from the donor catchment in the CAs space. This is also confirmed by the relationship that exists between the number of Mps transferred from the donor to the receptor catchments and the ASRIL factor plotted in Fig. 7. While the average FDCs uncertainty width (ASRIL) in both catchments groups tends to increase as the dissimilarity between the donor and the receptor catchments increases, catchments of the Pallas group show wider uncertainty interval than these of the Vène group. Another observation that can be made from Figs. 5 and 7 is that catchments that are very similar to each other have similar uncertain FDCs shape and very close ASRIL factor values (see also Table 4). This is the case for the Joncas and Lauze catchments in the Vène group and for the Nègues_Vacques and Aygues_Vacques catchments in the Pallas group. This suggests that high similarity between CAs may lead to similar hydrological responses and model prediction uncertainties of catchments that are under the same climatic and geographic region. However, this assumption is far to be validated in this work and needs to be further investigated and checked in future work with larger number of similar catchments or by simply gauging the catchments.

In order to check the consistency of the developed methodology in this work, attempts are conducted to investigate if relationships between Mps uncertainty of the donor catchment and the predicted uncertainty of the FDCs in the receptor catchments exist. This has been done through the calculation of the coefficient of variation (CV) of the transferred model parameter within each ungauged catchment. The CV, as it was described previously, can be used as a dimensionless measure of parameter

HESSD
10, 4951–5011, 2013

uncertainty (Bastola et al., 2008). The variability of the CV of Mps transferred to the ungauged catchments within each catchment group is given in Fig. 8. Results show that the CV of Mps varies between the catchments depending on the parameter itself and on the similarity distance between the receptor and the donor catchments.

In the Pallas catchment group, the CN2 and the SURLAG parameters show a clear variability in their corresponding CV values across the catchments. It is obvious that uncertainty in CN2 and SURLAG parameters increases from the closest (Negues-Vaques) to the furthest ungauged catchment (Fontanilles) from their respective donor catchment (Fig. 8a). Moreover, the variability trend of the CV of the CN2 parameter follows closely the trend of the ASRIL factor across the catchments, with a correlation coefficient of $R^2 = 0.66$ while the CV of the SURLAG parameter is less correlated to the ASRIL factor ($R^2 = 0.40$). In the Vène catchment group, 3 out of 10 transferred parameters show variable CV values across the catchments. These parameters are CN2, GW_DELAY and ALPHA_BF (Fig. 8b). While all the other remaining parameters show a constant CV at its maximum value across all the catchments, uncertainty in CN2, GW_DELAY and ALPHA_BF parameters increases progressively from the closest similar ungauged catchment (Joncas) to the furthest one, but in different trends. The variability of the CV of CN2 is well correlated to the ASRIL factor ($R^2 = 0.83$) while these of the GW_DELAY and ALPHA_BF parameters are less correlated to ASRIL ($R^2 = 0.545$ and 0. 540 for GW_DELAY and ALPHA_BF, respectively). These results suggest that relationships exist between the transferred parameter uncertainty and the predicted uncertainty width of the FDCs and between the CAs similarity distance and the predicted uncertainty in the ungauged catchment. The results are consistent with the proposed methodology in this work which is based on the principle that model prediction uncertainty intuitively increases as the dissimilarity in CAs between the donor and the receptor catchments increases. However, these results need to be interpreted with care and precaution. Indeed, the CV is calculated for each model parameter individually without taking simultaneously into account the uncertainty and the interactions between the other parameters while it is the whole parameters set that was transferred in the regionalization schemes. Furthermore, by relating the parameter CV to the model prediction uncertainty in ungauged catchment, it is assumed that linear relationship exists between parameter uncertainty and model prediction uncertainty at the ungauged catchments. However, this linearity is difficult to check and to establish because of the possible interdependency of the parameters, the non-linearity and the non-monotonicity of the hydrological model and because of other various sources of uncertainty (uncertainty in input and model structure). Moreover, model parameters that have steady CV across the ungauged catchments may contribute to model prediction uncertainty when they are transferred in a set of parameters values and, therefore, the CV of individual parameter may not reflect its real uncertainty. In addition to Mps, input and model structure uncertainty, regionalization procedures are known to have additional uncertainty on model prediction in ungauged catchments (Wagener et al., 2004; Heuvelmans et al., 2006; Bastola et al., 2008). In the proposed methodology it is assumed that uncertainty that stems from the regionalization schemes is propagated to model prediction in the ungauged catchment through the integration of the similarity measure in defining the Mps sets to be transferred from the donor to the receptor catchments. However, partitioning each uncertainty source and telling to which extent it can affect the model prediction is a very difficult task to perform.

5.3 Performances evaluation of the regionalization approach

5.3.1 Fit to observation

The 95 % uncertainty interval and the median of each flow percentiles values of the observed and the simulated FDCs for the ungauged catchments, where observed data are available, are constructed and plotted in Fig. 9. Only 4 ungauged catchments have some observed data that can be used to compare the results of the regionalization approach. According to the observed FDCs, ungauged catchments cease flowing at 50 to 60 % of the time while the predicted FDCs indicate that ungauged catchments flow for longer period between 60 and 100 % of the simulation time period reflecting

HESSD
10, 4951–5011, 2013

the ephemeral hydrological behaviour of the catchments (Fig. 9). The calculated NS coefficient between the observed and the simulated median flow percentiles and the average *p* factor values, corresponding to the average percentage of the observed flow percentile values bracketed in the predicted uncertainty flow percentile interval, are summarized in Table 5. Given the observation data available, the NS coefficient values are negative for the Soupié and Fontanilles catchments (NS = −0.131 and −0.144, respectively), indicating that the observed median values of the different flow percentiles are poorly reproduced by the model in these ungauged catchments. On the other hand, positive NS values of 0.169 and 0.518 are obtained in the Aygues_Vacques and in the Joncas catchments, respectively, showing better model prediction of the flow percentiles median values. While the simulated flow percentiles uncertainty intervals are able to bracket most of the observation data (Fig. 9 and Table 5), there is a clear tendency of the *p* factor increase with the decrease of the distance between the donor and the receptor catchment. As it was demonstrated previously, the average relative width of the uncertainty interval (ASRIL) increases as the dissimilarity between the donor and the receptor catchments increases. Therefore, more observation data are bracketed in the flow percentile uncertainty interval of the ungauged catchments that are located far from the donor catchment.

5.3.2 Fit to reality

The annual mass balance is calculated based on the average annual values of the different hydrological components that are computed by the SWAT model according to Eq. (6).

$$\mathrm{WYLD} = \mathrm{Surf\_}Q + \mathrm{Lat\_}Q + \mathrm{GW\_}Q - T\,\mathrm{Losses} \quad (6)$$

where WYLD is the net water yield to reach (mm), Surf_Q is the surface runoff (mm), Lat_Q is the lateral flow contribution to reach (mm), GW_Q is the groundwater discharge into the reach (mm) and T Losses is the amount of water removed from the tributary channel by transmission (mm).

HESSD
10, 4951–5011, 2013

The average annual water budget, its components and their corresponding uncertainty (calculated as the standard deviation) for each ungauged catchment are plotted in Fig. 10. The results of the regionalization approach suggest that surface runoff is the major component of the water budget (65 % in average) followed by the lateral flow (22.7 % in average) and by the groundwater flow (12.3 % in average). However, all the hydrological balance components are estimated with large uncertainty. For instance, about 65% of the WYLD uncertainty is attributed to the uncertainty of the estimated surface runoff (Surf_*Q*). In the SWAT model, Surf_*Q* is estimated using the modified Soil Conservation Service (SCS) curve number (CN) method which depends on the soil moisture and land use cover. Therefore, any uncertainty in the soil and land use cover is translated to the associated curve number and affects the predicted Surf_*Q*. Moreover, in SWAT the runoff coefficient is calculated as the ratio of runoff volume to rainfall. Therefore, uncertainty of the latter can affect the predicted peak flow which in turn affects the predicted Surf_*Q*.

The groundwater component (GW_*Q*) has more important average contribution rate to the total water budget in the Vène catchments group (Joncas, Lauze, Aiguilles and Mayroual) with an average of 11.71 %, than in the Pallas catchments group (Nègues_Vacques, Aygues_Vacques, Soupié and Fontanilles), with an average of 6.47 %. In addition, GW_*Q* within the Pallas catchments group occurs intermittently, while it seems more sustained but also more uncertain within the Vène catchments group (Fig. 10). Because of the different sources of uncertainty (e.g. precipitation, evapotranspiration, uncertainty in groundwater parameters) and the rainfall seasonal variability, the groundwater volume and its level of fluctuation are estimated with uncertainty that is translated into an uncertain GW_*Q*. These results suggest that streamflow in the Vène catchments group (corresponding more or less to the eastern part of the Thau catchment, see Fig. 1) is more influenced by the groundwater flow contribution than in the Pallas catchments group (corresponding to the central and western part of the Thau catchment). However, validation of this result is not straightforward since no information or data on groundwater are available in the study area and more

HESSD
10, 4951–5011, 2013

hydrogeological measurements are required to check the results and to reduce the groundwater discharge uncertainty.

About 2.5 % of the total water budget is lost via leaching through the stream bed (*T* Losses). This type of losses is more important in the Pallas catchments group (5.3 %), than in the Vène catchment group (1.37 %) (Fig. 10). Transmission losses become more important when GW_*Q* decreases and vice versa. Because the SWAT model creates more sustained shallow aquifer with larger water storage in the eastern part than in the western part of the Thau catchment, the Vène catchments group is gaining much more water through baseflow (GW_*Q* + Lat_*Q*) and, thus, there is smaller loss of water through channel transmission in that case. However, besides the depth of water stored in the shallow aquifer, other geomorphologic parameters (e.g. the width and length of the channel bed, etc.) and hydraulic parameters (e.g. effective hydraulic conductivity of the river bed (Ch_*K*), geologic nature of the channel material) can affect the transmission losses amount. For example, for catchments where the groundwater level is beyond the river bed, the CH_*K* value should be equal to zero (van Griensven et al., 2012) and should not be too high in humid catchments. Uncertainty in the estimated transmission losses can stem from the uncertainty of the physical features of the catchments introduced through the GIS data and used by SWAT to derive the channel geomorphological characteristics and from the uncertainty of the CH_*K* parameter.

5.3.3 Fit to geography

This criterion is used here to assess the performances of the regionalization procedure in reproducing the actual spatial distribution of the soil moisture in the Thau catchment. Baghdadi et al. (2012) proposed a method to estimate the volumetric soil moisture from RADARSAT-2 image (space Synthetic Aperture Radar "SAR" sensor) for bare agricultural fields or fields with thin vegetation cover over the Thau basin for ten dates between November 2010 and March 2011. Their estimated soil moisture values showed a good agreement with the measured in situ soil moisture with a RMSE = 0.065 $cm^3\,cm^{-3}$ (see Baghdadi et al., 2012, for details). These estimated soil

HESSD
10, 4951–5011, 2013

moisture maps, referred hereafter as “observed” soil moisture, are compared to the soil moisture derived from the regionalization results which are referred hereafter as predicted soil moisture. Since the “observed” soil moisture maps are available only for three different dates (18 November, 4 and 12 December 2010) within the model simulation period, the comparison between the “observed” and the predicted soil moistures is restricted to these 3 dates. Figure 11 shows the spatial distribution of the predicted and the observed soil moisture for three different dates at the Thau catchment. The predicted soil moisture is spatially correlated to the “observed” one but with different degree of satisfaction. The latter can be broadly and arbitrary set to good, satisfactory and poor based on the graphical investigation of Fig. 11. Good spatial correlation between the distribution of the predicted and the “observed” soil moisture is obtained at the Vène, Aiguilles and Fontanilles catchments, while it can be considered as satisfactory for the Joncas, Lauze, Pallas and Soupié and poor for the Aygues_Vacques, Mayroual and Nègues_Vacques catchments. Overall, the predicted soil moisture has an acceptable spatial distribution with the “observed” one which is more clear in the eastern part (corresponding to the Vène catchments group) than in the western part (corresponding to the Pallas catchments group) of the Thau catchment.

The predicted soil moisture values on the three different dates at the Thau catchment are also compared to the “observed” ones. Table 6 presents some statistical characteristics of the 95 % “observed” and predicted soil moisture values on the three dates at the Thau catchment. The predicted soil moisture values ranges are slightly larger than the “observed” ones. The variability of the predicted soil moisture on a given day is larger as this day is preceded by wet days (Table 6). Nevertheless, the median and the mean of the “observed” and predicted soil moisture values are in a good agreement. However, the comparison of the “observed” and predicted soil moisture values is not straightforward since the model is predicting the soil moisture at the HRU scale for soils with different vegetation type cover, while the “observed” soil moisture values are made up for bare soils or soils with thin vegetation cover. In addition, “observed” soil moisture values are made up for the top 5 to 10 cm of the soil profile whereas the

HESSD
10, 4951–5011, 2013

predicted ones might be estimating by SWAT for the entire soil layer that can be much more than 10 cm depth.

6 Summary and conclusions

This study examined the possibility of the Soil and Water Assessment Tool (SWAT) model to accurately predict the daily discharge at gauged and ungauged catchments within an uncertainty framework. The model was implemented on a Mediterranean catchment, called the Thau catchment located in southern France. Model calibration and parameters uncertainty were conducted simultaneously using the GLUE method (Beven and Binley, 1992) on two gauged subcatchments of the Thau watershed, referred to as the Vène and the Pallas catchment.

We first questioned whether the selected hydrological model is suitable for reproducing the hydrology of the study area. The model showed good performances in reproducing the daily observed discharge of the Vène and the Pallas catchments with NS coefficient higher than 0.70. The model was able to cover more than 60 % of the observation discharge data of each catchment in its 95 % prediction uncertainty interval. However, the model prediction uncertainty was large in both study sites especially in the Vène catchment due to the presence of the karstic features. The results suggested also that SWAT can be applied to karstified watershed but with some constraints and limitations unless its original structure is modified to explicitly handle these karstic features.

We subsequently questioned whether the selected hydrological model is able to predict the discharge at ungauged catchments. We analyzed this question through the transfer of the SWAT model parameter sets from the gauged catchments (Vène and Pallas) to the other ungauged catchments of the Thau watershed. A regionalization approach based on a physical similarity measure (similarity in physical catchments attributes) was adopted to cluster the ungauged catchments. To transfer the model parameter sets from gauged to ungauged catchment, a new methodology was developed where the similarity measure was used as a threshold to select the numbers of the candidate model parameter sets to be transferred from the gauged to the ungauged catchment. Results showed that within the same catchments cluster, ungauged catchments can exhibit similar hydrologic behavior if they exhibit high degree of similarity in their physical attributes and have received similar model parameter sets. Similar ungauged catchments showed higher similarity at the predicted FDCs high flow percentiles than at low flow percentiles. The high variability of the predicted low flow values was attributed to the predicted low mean values of the flow percentiles rather than to the geology or to the catchment drainage area.

The performance of the regionalization method at the ungauged catchments was assessed through statistical and field reality criteria. The predicted median flow percentiles, given the available observed data, were poorly to acceptable reproduced by the model. The predicted water balance revealed the prevailing of the surface runoff component in the hydrology of the ungauged catchments. The predicted soil moisture was satisfactory spatially correlated to the "observed" one for some given dates. The findings suggest that the SWAT model parameters can be regionalized to predict discharge at ungauged catchments and the results can fit the reality of the study case. However, thorough evaluation and criticism of its performances is constrained by the availability of the observation data at the ungauged catchments. Therefore, other evaluation criteria such as fit to reality and fit to geography can be used to describe the model performances in these ungauged catchments.

We also showed in this work how parameter uncertainty can affect model prediction uncertainty at ungauged catchment through the regionalization of the model parameters. The assumptions behind the developed methodology were that similar catchments (similar in their physical attributes) are hydrologically similar and that model prediction uncertainty increases as the dissimilarity between the donor and the receptor catchment decreases. The developed methodology allows propagating model parameter uncertainty proportionally to the similarity measure. Furthermore, the integration of the similarity measure in the function used to calculate the threshold value makes

HESSD
10, 4951–5011, 2013

the selection of the donor catchment parameter sets more objective than the traditional approach which is based on modeler subjective choice of the threshold value. It was shown that model prediction uncertainty was influenced by the similarity distance between the donor and the receptor catchment; wider prediction uncertainty is obtained as the dissimilarity between the donor and the receptor catchment increases. It was also shown that within the same climatic and geographic region, catchments that are very similar to each other and have received similar model parameter sets exhibit similar degree of prediction uncertainty. In addition, the findings showed that the selected threshold values and, hence, the number and the uncertainty of the parameters transferred can affect the prediction uncertainty at the ungauged catchment. If a higher degree of similarity exists between the donor and the receptor catchments, then a higher threshold value is selected and a lower uncertainty of model parameters is propagated to the ungauged catchment which yields to lower prediction uncertainty in the ungauged catchment. Otherwise, a lower threshold value is selected and a wider uncertain parameter sets are transferred which will yield a larger uncertain model prediction at the target catchment. However, it is not pretended with these results that uncertainty in the transferred parameter sets is the only one driving the uncertainty source for model prediction uncertainty at the ungauged catchment. As it was demonstrated by the results, although the relationship between the transferred model parameters uncertainty and model prediction uncertainty at the ungauged catchments exists, this relationship is far to be linear due to the non-linearity of the hydrological model, to the possible correlation between the parameters, to the equifinality problem, to the non-identifiable parameters and to other sources of uncertainty (e.g. model structure, inputs uncertainty) that are difficult to be simultaneously taken into account. This suggests that, besides parameter uncertainty all sources of uncertainty should be considered in an integrated regionalization framework while transferring the model parameters from the donor to the receptors catchments.

To our knowledge, a hydrological study of the entire Thau catchment was never done before. Therefore, building on the regionalization approach, this work can be considered as a starting point for further research study of hydrological issues in this catchment.

We think that the developed methodology in this work provides more objectivity in the selection of the transferrable model parameters sets for estimating the discharge at the ungauged catchments. This can reduce a part of the additional uncertainty that can be introduced by the user through his subjective selection of the transferrable model parameters. However, some subjective choices are inevitable such as the choice of the similarity measure and the selection of the catchment attributes which can have an additional source of uncertainty. We think also that the speculation behinds the developed methodology such as model prediction uncertainty at the ungauged catchments increases as the dissimilarity between the donor and the receptor catchment increases is appealing, reasonable and provides more reliable prediction uncertainty at the ungauged catchment than the traditional approach. The method is easy and can be replicated with any model parameters transfer approach for estimating flow at ungauged catchments within an uncertainty propagation framework.

Acknowledgements. This work was funded by the IDB (Islamic development Bank) under its Ph.D. Merit Scholarship program. The work has been conducted in the context of the European project CLIMB (Climate induced changes on the hydrology of Mediterranean Basins). Authors thank Egis eau, the Syndicat Mixte du Bassin du Thau and Ifremer for providing most of the data.

References

Abbaspour, K. C., van Genuchten, M. T., Schulin, R., and Schläppi, E.: A sequential uncertainty domain inverse procedure for estimating subsurface flow and transport parameters, Water Resour. Res., 33, 1879–1892, doi:10.1029/97wr01230, 1997.

Afinowicz, J. D., Munster, C. L., and Wilcox, B. P.: Modeling effect of brush management on the Rangeland water budget: Edwards Plateau, Texas, J. Am. Water. Resour. As., 41, 181–193, doi:10.1111/j.1752-1688.2005.tb03727.x, 2005.

HESSD
10, 4951–5011, 2013
Uncertainty analysis in model parameters regionalization
H. Sellami et al.

Aquilina, L., Ladouche, B., Doerfliger, N., Seidel, J. L., Bakalowicz, M., Dupuy, C., and Le Strat, P.: Origin, evolution and residence time of saline thermal fluids (Balaruc springs, southern France): implications for fluid transfer across the continental shelf, Chem. Geol., 192, 1–21, doi:10.1016/S0009-2541(02)00160-2, 2002.

Arabi, M., Govindaraju, R. S., and Hantush, M. M.: A probabilistic approach for analysis of uncertainty in the evaluation of watershed management practices, J. Hydrol., 333, 459–471, doi:10.1016/j.jhydrol.2006.09.012, 2007.

Arnold, J. G., Srinivasan, R., Muttiah, R. S., and Williams, J. R.: Large area hydrological modeling and assessment Part I: Model development 1, J. Am. Water. Resour. As., 34, 73–89, doi:10.1111/j.1752-1688.1998.tb05961.x, 1998.

Baffaut, C. and Benson, V. W.: Modeling flow and pollutant transport in a karst watershed with SWAT, T. ASABE, 52, 469–479, 2009.

Baghdadi, N., Cresson, R., El Hajj, M., Ludwig, R., and La Jeunesse, I.: Estimation of soil parameters over bare agriculture areas from C-band polarimetric SAR data using neural networks, Hydrol. Earth Syst. Sci., 16, 1607–1621, doi:10.5194/hess-16-1607-2012, 2012.

Bárdossy, A.: Calibration of hydrological model parameters for ungauged catchments, Hydrol. Earth Syst. Sci., 11, 703–710, doi:10.5194/hess-11-703-2007, 2007.

Bastola, S., Ishidaira, H., and Takeuchi, K.: Regionalisation of hydrological model parameters under parameter uncertainty: A case study involving TOPMODEL and basins across the globe, J. Hydrol., 357, 188–206, doi:10.1016/j.jhydrol.2008.05.007, 2008.

Benham, B. L., Baffaut, C., Zeckoski, R. W., Mankin, K. R., Pachepsky, Y. A., Sadeghi, A. M., Brannan, K. M., Soupir, M. L., and Habersack, M. J.: Modelling bacteria fate and transport in watersheds to support TMDLS, T. ASABE, 49, 987–1002, 2006.

Beven, K.: On the future of distributed modelling in hydrology, Hydrol. Process., 14, 3183–3184, doi:10.1002/1099-1085(200011/12)14:16/17<3183::AID-HYP404>3.0.CO;2-K, 2000.

Beven, K.: A manifesto for the equifinality thesis, J. Hydrol., 320, 18–36, doi:10.1016/j.jhydrol.2005.07.007, 2006.

Beven, K. and Binley, A.: The future of distributed models: Model calibration and uncertainty prediction, Hydrol. Process., 6, 279–298, doi:10.1002/hyp.3360060305, 1992.

Beven, K. and Freer, J.: Equifinality, data assimilation, and uncertainty estimation in mechanistic modelling of complex environmental systems using the GLUE methodology, J. Hydrol., 249, 11–29, 2001.

Blasone, R.-S., Madsen, H., and Rosbjerg, D.: Uncertainty assessment of integrated distributed hydrological models using GLUE with Markov chain Monte Carlo sampling, J. Hydrol., 353, 18–32, doi:10.1016/j.jhydrol.2007.12.026, 2008.

Castellarin, A., Galeati, G., Brandimarte, L., Montanari, A., and Brath, A.: Regional flow-duration curves: reliability for ungauged basins, Adv. Water Resour., 27, 953–965, doi:10.1016/j.advwatres.2004.08.005, 2004.

Chahinian, N., Tournoud, M.-G., Perrin, J.-L., and Picot, B.: Flow and nutrient transport in intermittent rivers: a modelling case-study on the Vène River using SWAT 2005, Hydrolog. Sci. J., 56, 268–287, doi:10.1080/02626667.2011.559328, 2011.

Coffey, M. E., Workman, S. R., Taraba, J. L., and Fogle, A. W.: Statistical procedures for evaluating daily and monthly hydrologic model predictions, T.e ASABE, 47, 59–68, 2004.

Dotto, C. B., Mannina, G., Kleidorfer, M., Vezzaro, L., Henrichs, M., McCarthy, D. T., Freni, G., Rauch, W., and Deletic, A.: Comparison of different uncertainty techniques in urban stormwater quantity and quality modelling, Water Res., 46, 2545–2558, doi:10.1016/j.watres.2012.02.009, 2012.

Duan, Q., Sorooshian, S., and Gupta, V.: Effective and efficient global optimization for conceptual rainfall-runoff models, Water Resour. Res., 28, 1015–1031, doi:10.1029/91wr02985, 1992.

Eckhardt, K., Fohrer, N., and Frede, H.-G.: Automatic model calibration, Hydrol. Process., 19, 651–658, doi:10.1002/hyp.5613, 2005.

Freer, J., Beven, K., and Ambroise, B.: Bayesian Estimation of Uncertainty in Runoff Prediction and the Value of Data: An Application of the GLUE Approach, Water Resour. Res., 32, 2161–2173, doi:10.1029/95WR03723, 1996.

Freni, G. and Mannina, G.: Bayesian approach for uncertainty quantification in water quality modelling: The influence of prior distribution, J. Hydrol., 392, 31–39, doi:10.1016/j.jhydrol.2010.07.043, 2010.

Gallart, F., Amaxidis, Y., Botti, P., CanÈ, G., Castillo, V., Chapman, P., Froebrich, J., GarcÍA-Pintado, J., Latron, J., Llorens, P., Porto, A. L., Morais, M., Neves, R., Ninov, P., Perrin, J.-L., Ribarova, I., Skoulikidis, N., and Tournoud, M.-G.: Investigating hydrological regimes and processes in a set of catchments with temporary waters in Mediterranean Europe, Hydrolog. Sci. J., 53, 618–628, doi:10.1623/hysj.53.3.618, 2008.

Gassman, P. W., Reyes, M. R., Green, C. H., and Arnold, J. G.: The Soil and Water Assessment Tool: Historical development, applications and future research directions, T. ASABE, 50, 1211–1250, 2007.
Gitau, M. W. and Chaubey, I.: Regionalization of SWAT Model Parameters for Use in Ungauged Watersheds, Water, 2, 849–871, 2010.
Gong, Y., Shen, Z., Hong, Q., Liu, R., and Liao, Q.: Parameter uncertainty analysis in watershed total phosphorus modeling using the GLUE methodology, Agriculture, Ecosys. Environ., 142, 246–255, doi:10.1016/j.agee.2011.05.015, 2011.
He, Y., Bárdossy, A., and Zehe, E.: A review of regionalisation for continuous streamflow simulation, Hydrol. Earth Syst. Sci., 15, 3539–3553, doi:10.5194/hess-15-3539-2011, 2011.
Heuvelmans, G., Muys, B., and Feyen, J.: Analysis of the spatial variation in the parameters of the SWAT model with application in Flanders, Northern Belgium, Hydrol. Earth Syst. Sci., 8, 931–939, doi:10.5194/hess-8-931-2004, 2004.
Heuvelmans, G., Muys, B., and Feyen, J.: Regionalisation of the parameters of a hydrological model: Comparison of linear regression models with artificial neural nets, J. Hydrol., 319, 245–265, doi:10.1016/j.jhydrol.2005.07.030, 2006.
Jin, X., Xu, C.-Y., Zhang, Q., and Singh, V. P.: Parameter and modeling uncertainty simulated by GLUE and a formal Bayesian method for a conceptual hydrological model, J. Hydrol., 383, 147–155, doi:10.1016/j.jhydrol.2009.12.028, 2010.
La Jeunesse, I., Deslous-Paoli, J. M., Ximénès, M. C., Cheylan, J. P., Mende, C., Borrero, C., and Scheyer, L.: Changes in point and non-point sources phosphorus loads in the Thau catchment over 25 years (Mediterranean Sea – France), Hydrobiologia, 475–476, 403–411, doi:10.1023/a:1020351711877, 2002.
Mantovan, P. and Todini, E.: Hydrological forecasting uncertainty assessment: Incoherence of the GLUE methodology, J. Hydrol., 330, 368–381, doi:10.1016/j.jhydrol.2006.04.046, 2006.
Masih, I., Uhlenbrook, S., Maskey, S., and Ahmad, M. D.: RFegionalization of a conceptual rainfall–runoff model based on similarity of the flow duration curve: A case study from the semi-arid Karkheh basin, Iran, J. Hydrol., 391, 188–201, doi:10.1016/j.jhydrol.2010.07.018, 2010.
McIntyre, N., Lee, H., Wheater, H., Young, A., and Wagener, T.: Ensemble predictions of runoff in ungauged catchments, Water Resour. Res., 41, W12434, doi:10.1029/2005WR004289, 2005.

HESSD
10, 4951–5011, 2013

Title Page
Abstract | Introduction
Conclusions | References
Tables | Figures
◀◀ | ▶▶
◀ | ▶
Back | Close
Full Screen / Esc
Printer-friendly Version
Interactive Discussion

Merz, R. and Blöschl, G.: Regionalisation of catchment model parameters, J. Hydrol., 287, 95–123, doi:10.1016/j.jhydrol.2003.09.028, 2004.
Montanari, A.: Large sample behaviors of the generalized likelihood uncertainty estimation (GLUE) in assessing the uncertainty of rainfall-runoff simulations, Water Resour. Res., 41, W08406, doi:10.1029/2004WR003826, 2005.
Muleta, M. K. and Nicklow, J. W.: Sensitivity and uncertainty analysis coupled with automatic calibration for a distributed watershed model, J. Hydrol., 306, 127–145, doi:10.1016/j.jhydrol.2004.09.005, 2005.
Nathan, R. J. and McMahon, T. A.: Identification of homogeneous regions for the purposes of regionalisation, J. Hydrol., 121, 217–238, 1990.
Neitsh, S. L., Arnold, J. G., Kiniry, J. R., Srinivasan, R., and Williams, J. R.: Soil and Water Assessment Tool input/output file documentation, version 2005, Temple, Texas: Grassland, Soil and Water Research Laboratory, Agricultural Research Service, 2005.
Oudin, L., Andréassian, V., Perrin, C., Michel, C., and Le Moine, N.: Spatial proximity, physical similarity, regression and ungaged catchments: A comparison of regionalization approaches based on 913 French catchments, Water Resour. Res., 44, W03413, doi:10.1029/2007WR006240, 2008.
Parajka, J., Merz, R., and Blöschl, G.: A comparison of regionalisation methods for catchment model parameters, Hydrol. Earth Syst. Sci., 9, 157–171, doi:10.5194/hess-9-157-2005, 2005.
Perrin, J.-L. and Tournoud, M.-G.: Hydrological processes controlling flow generation in a small Mediterranean catchment under karstic influence, Hydrolog. Sci. J., 54, 1125–1140, doi:10.1623/hysj.54.6.1125, 2009.
Plus, M., La Jeunesse, I., Bouraoui, F., Zaldivar, J., Chapelle, A., and Lazure, P.: Modelling water discharges and nitrogen inputs into a Mediterranean lagoon-Impact on the primary production, Ecol. Model., 193, 69–89, doi:10.1016/j.ecolmodel.2005.07.037, 2006.
Sellami, H., La Jeunesse, I., Benabdallah, S., and Vanclooster, M.: Parameter and rating curve uncertainty propagation analysis of the SWAT model for two small Mediterranean watersheds, Hydrolog. Sci. J., accepted, 2013.
Setegn, S. G., Srinivasan, R., Melesse, A. M., and Dargahi, B.: SWAT model application and prediction uncertainty analysis in the Lake Tana Basin, Ethiopia, Hydrol. Process., 24, 357–367, doi:10.1002/hyp.7457, 2009.

HESSD
10, 4951–5011, 2013

Shen, Z. Y., Chen, L., and Chen, T.: Analysis of parameter uncertainty in hydrological and sediment modeling using GLUE method: a case study of SWAT model applied to Three Gorges Reservoir Region, China, Hydrol. Earth Syst. Sci., 16, 121–132, doi:10.5194/hess-16-121-2012, 2012.

Shrestha, D. L., Kayastha, N., and Solomatine, D. P.: A novel approach to parameter uncertainty analysis of hydrological models using neural networks, Hydrol. Earth Syst. Sci., 13, 1235–1248, doi:10.5194/hess-13-1235-2009, 2009.

Sivapalan, M., Takeuchi, K., Franks, S. W., Gupta, V. K., Karambiri, H., Lakshmi, V., Liang, X., McDonnell, J. J., Mendiondo, E. M., O'Connell, P. E., Oki, T., Pomeroy, J. W., Schertzer, D., Uhlenbrook, S., and Zehe, E.: IAHS Decade on Predictions in Ungauged Basins (PUB), 2003–2012: Shaping an exciting future for the hydrological sciences, Hydrolog. Sci. J., 48, 857–880, doi:10.1623/hysj.48.6.857.51421, 2003.

Smakhtin, V. U.: Low flow hydrology: a review, J. Hydrol., 240, 147–186, doi:10.1016/S0022-1694(00)00340-1, 2001.

Spruill, C. A., Workman, R. S., and Taraba, J. L.: Simulation of daily and monthly stream discharge from small watersheds using the SWAT model, T. Am. Soc. Agr. Eng., 43, 1431–1439, 2000.

van Griensven, A., Meixner, T., Grunwald, S., Bishop, T., Diluzio, M., and Srinivasan, R.: A global sensitivity analysis tool for the parameters of multi-variable catchment models, J. Hydrol., 324, 10–23, doi:10.1016/j.jhydrol.2005.09.008, 2006.

van Griensven, A., Ndomba, P., Yalew, S., and Kilonzo, F.: Critical review of SWAT applications in the upper Nile basin countries, Hydrol. Earth Syst. Sci., 16, 3371–3381, doi:10.5194/hess-16-3371-2012, 2012.

Vandewiele, G. L. and Elias, A.: Monthly water balance of ungauged catchments obtained by geographical regionalization, J. Hydrol., 170, 277–291, 1995.

Viola, F., Noto, L. V., Cannarozzo, M., and La Loggia, G.: Daily streamflow prediction with uncertainty in ephemeral catchments using the GLUE methodology, Phys. Chem. Earth, 34, 701–706, doi:10.1016/j.pce.2009.06.006, 2009.

Vogel, R. M. and Fennessey, N. M.: Flow-Duration Curves 2. New Interpretation and Con?dence-Intervals, J. Water Res. Pl.-ASCE, 120, 485–504, 1994.

Vogel, R. M. and Fennessey, N. M.: Flow Duration Curve II: A review of applications in water resources planning, JAWRA, J. Am. Water Resour. Ass., 31, 1029–1039, doi:10.1111/j.1752-1688.1995.tb03419.x, 1995.

Vrugt, J. A., ter Braak, C. J. F., Clark, M. P., Hyman, J. M., and Robinson, B. A.: Treatment of input uncertainty in hydrologic modeling: Doing hydrology backward with Markov chain Monte Carlo simulation, Water Resour. Res., 44, doi:10.1029/2007wr006720, 2008.

Wagener, T. and Wheater, H. S.: Parameter estimation and regionalization for continuous rainfall-runoff models including uncertainty, J. Hydrol., 320, 132–154, 2006.

Wagener, T., Wheater, H. S., and Gupta, H. V.: Rainfall-Runoff Modelling in Gauged and Ungauged Catchments, Imperial College Press, London, 300 pp., 2004.

Wagener, T., Sivapalan, M., Troch, P., and Woods, R.: Catchment Classification and Hydrologic Similarity, Geography Compass, 1, 901–931, doi:10.1111/j.1749-8198.2007.00039.x, 2007.

Xiong, L. and O'Connor, K. M.: An empirical method to improve the prediction limits of the GLUE methodology in rainfall-runoff modeling, J. Hydrol., 349, 115–124, 2008.

Yadav, M., Wagener, T., and Gupta, H.: Regionalization of constraints on expected watershed response behavior for improved predictions in ungauged basins, Adv. Water. Resour, 30, 1756–1774, doi:10.1016/j.advwatres.2007.01.005, 2007.

Yang, J., Reichert, P., Abbaspour, K. C., Xia, J., and Yang, H.: Comparing uncertainty analysis techniques for a SWAT application to the Chaohe Basin in China, J. Hydrol., 358, 1–23, doi:10.1016/j.jhydrol.2008.05.012, 2008.

Zhang, X., Srinivasan, R., Zhao, K., and Liew, M. V.: Evaluation of global optimization algorithms for parameter calibration of a computationally intensive hydrologic model, Hydrol. Process., 23, 430–441, doi:10.1002/hyp.7152, 2009.

HESSD

10, 4951–5011, 2013

Table 1. Description of the catchments attributes.

Catchment name	Drainage area (km^2)	Mean elevation (m)	Average slope (%)	Vineyards (%)	Non-agr vegetation (%)	Dominant Soil texture	Geology (surface %)
Vène	67	94.29	8.47	12.30	64	SA-L	JL-MM
Pallas	54	71.33	7	20.35	45.48	S-L	JL-MM
Lauze	9.25	64.22	8.16	8.027	64	S-L	JL-MM
Aiguilles	3.42	60	5.87	0.34	83.27	S-C-L	JL-MM
Joncas	4.14	74.45	6.56	2.5	84.22	S-C-L	JL-MM
Aygues_Vacques	12.34	29.52	3.56	14.40	37.33	S-L	MM
Negue	28.50	53.52	4	29.18	41.32	L	MM
Mayroual	5.10	20.45	2.55	48.63	25.15	L	MM
Soupié	15.82	43.38	3.79	35.88	45	L	MM
Fontanilles	7.40	21.21	2.38	31.39	27.11	L	MM

Soil code: SA-L: sandy loam, S-L: silty loam, S-C-L: silty clayey loam and L: loam. Geology code: JL, Jurassic Limestone; MM, Miocene Marls.

HESSD
10, 4951–5011, 2013

Uncertainty analysis in model parameters regionalization

H. Sellami et al.

HESSD
10, 4951–5011, 2013

Uncertainty analysis in model parameters regionalization

H. Sellami et al.

Table 2. The selected sensitive parameters, their initial range and their SA ranking result.

		SA ranking		
Name	A priori distribution	Vène	Pallas	Parameter description [unit]
ALPHA_BF	U [0.1–1]	1	2	Base-flow alpha factor [days]
GW_DELAY	U [0–500]	3	7	Groundwater delay [days]
GW_REVAP	U [0.02–0.2]	6	8	Groundwater “revap” coefficient [none]
GWQMN	U [0–5000]	2	1	Threshold water depth in the shallow aquifer for flow [mm]
CN2*	U [0.1–0.9]	9	3	Initial SCS CN II value [none]
ESCO	U [0.1–1]	8	6	Soil evaporation compensation factor [none]
EPCO	U [0–1]	7	9	Plant uptake compensation factor [none]
SURLAG	U [1–24]	10	10	Surface runoff lag time [days]
CH_N2	U [0.1–0.3]	5	5	Manning’s n value for main channel [none]
CH_K2	U [1–150]	4	4	Channel effective hydraulic conductivity [mm h^{-1}]

Note: U means uniform distribution. * Means fraction of variation by which the initial value of the parameter is changed.

Table 3. Results of catchments clustering and number of Mps transferred from the donor to the receptor catchment based on the similarity measure.

	Donor catchment	Receptor catchment	Similarity	Threshold (Thresh)	% of Mps
Catchments cluster	Vène	Joncas	0.71	0.50	44.10
		Lauze	0.70	0.49	46.95
		Aiguilles	0.66	0.46	54.62
		Mayroual	0.36	0.25	89.18
	Pallas	Nègues_Vacques	0.88	0.66	16.60
		Aygues_Vacques	0.71	0.54	85.16
		Soupié	0.70	0.53	86.47
		Fontanilles	0.50	0.38	96.52

Note: the %Mps corresponds to the percentage of the transferred Mps out of 10 000.

HESSD
10, 4951–5011, 2013

Table 4. Measure of the ASRIL factor of the predicted FDCs uncertainty intervals in the ungauged catchments.

	Donor catchment	
Ungauged catchment	Vène	Pallas
Lauze	0.018	–
Aiguilles	0.031	–
Joncas	0.019	–
Mayroual	0.207	–
Fontanilles	–	0.196
Aygues_Vacques	–	0.117
Negue_Vaques	–	0.113
Soupié	–	0.169

HESSD
10, 4951–5011, 2013

Table 5. Statistical criteria of the regionalization approach results.

Catchment	Aygues_Vacques	Soupié	Fontanilles	Joncas
NS	0.169	−0.131	−0.144	0.518
p factor (%)	18	65	73	87

Discussion Paper | Discussion Paper | Discussion Paper | Discussion Paper |

HESSD

10, 4951–5011, 2013

Uncertainty analysis in model parameters regionalization

H. Sellami et al.

Table 6. Statistical criteria of the "observed" and predicted soil moisture values on three dates at the Thau catchment.

	"Observed" soil moisture ($cm^3\,cm^{-3}$)			Predicted soil moisture ($cm^3\,cm^{-3}$)		
95 %	18 Nov 2010	4 Dec 2010	12 Dec 2010	18 Nov 2010	4 Dec 2010	12 Dec 2010
Prec.*	2.2	0.6	0	2.2	0.6	0
Min–Max	0.08–0.27	0.10–0.26	0.03–0.19	0.08–0.33	0.04–0.30	0.01–0.28
Median	0.167	0.162	0.07	0.142	0.102	0.07
Mean	0.169	0.166	0.08	0.167	0.127	0.09

Note: * Prec. is the cumulative precipitation in (mm) from the 3 previous days to the selected date.

HESSD
10, 4951–5011, 2013

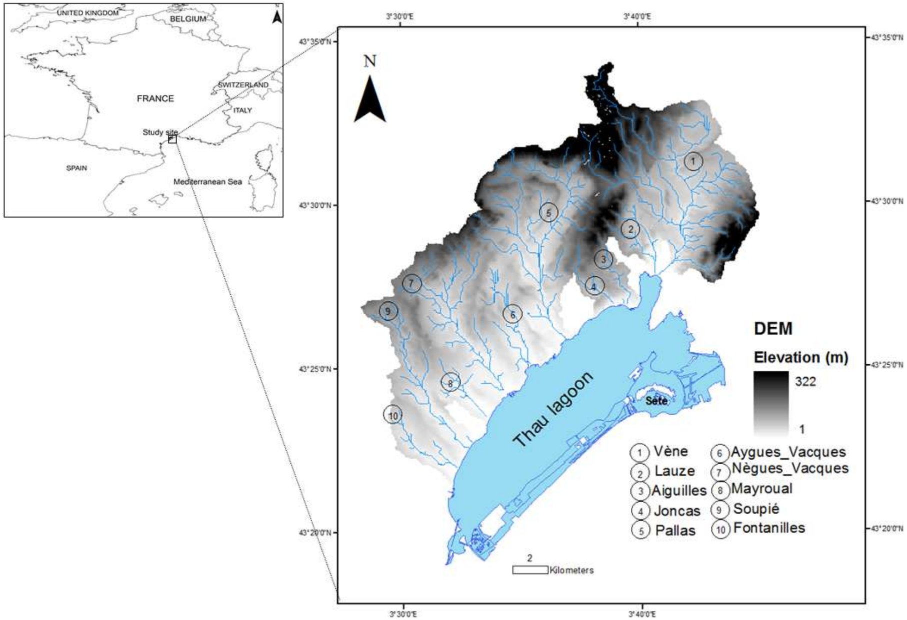

Fig. 1. Location of the Thau catchment, topography and its sub-watersheds.

HESSD
10, 4951–5011, 2013

Uncertainty analysis in model parameters regionalization

H. Sellami et al.

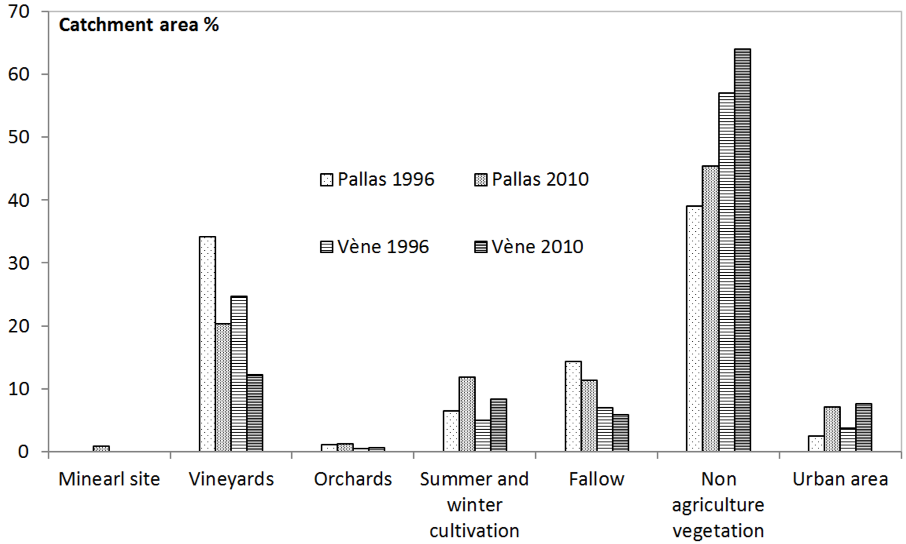

Fig. 2. Land use distribution in the Vène and in the Pallas watersheds for 1996 and 2010.

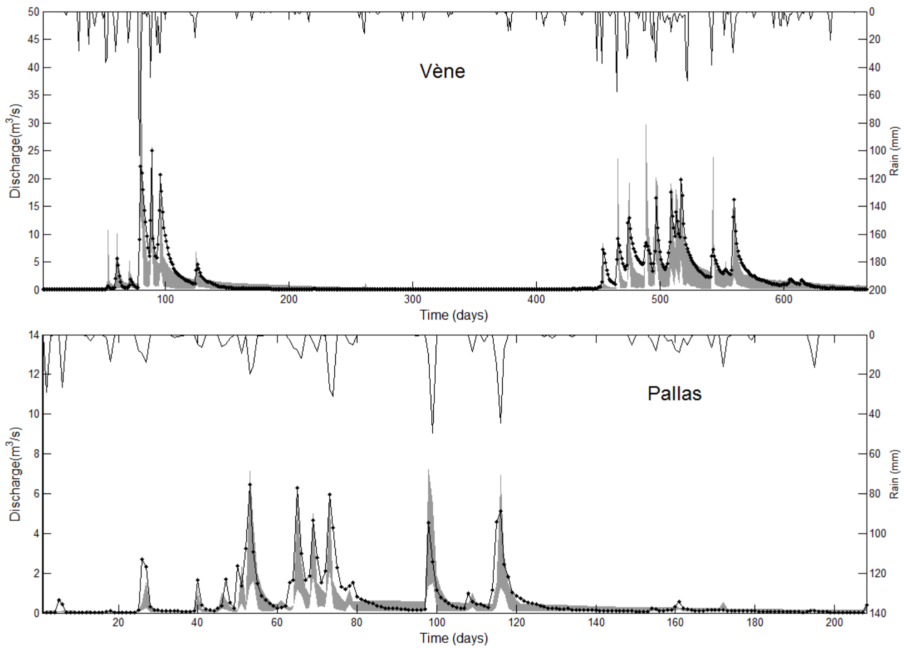

Fig. 3. GLUE prediction uncertainty bounds for the Vène and the Pallas catchment. The grey shaded area is the 95 % prediction uncertainty interval and the black dotted line corresponds to the observed discharge.

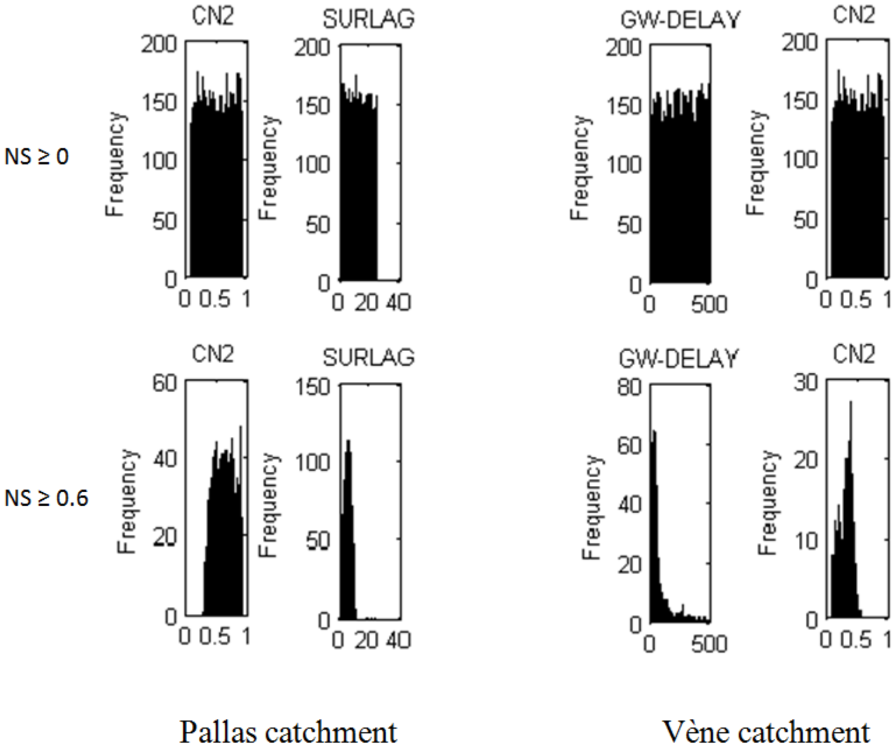

Fig. 4. Example of the effect of the threshold value on the posterior parameter distribution derived by GLUE.

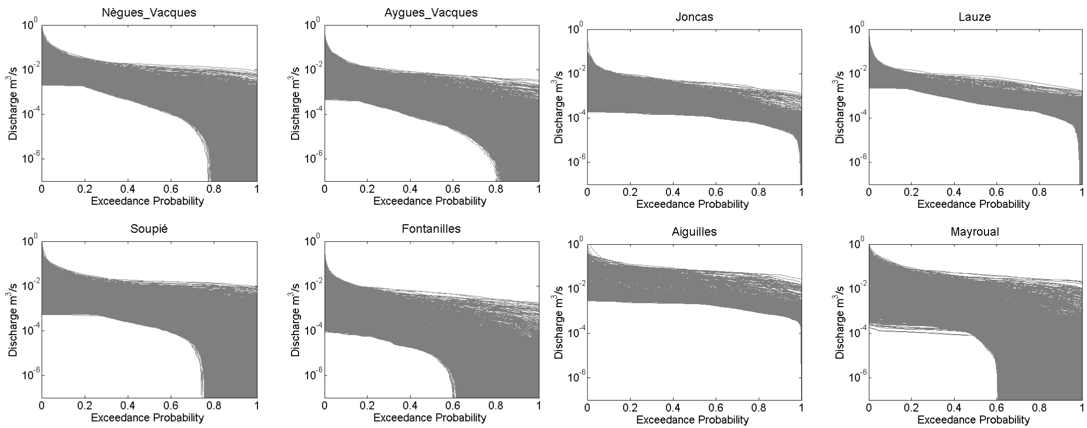

(a) Uncertain simulated FDCs for the Pallas catchments group

(b) Uncertain simulated FDCs for the Vène catchments group

Fig. 5. Simulated uncertain FDCs for the ungauged catchments based on model parameters regionalization.

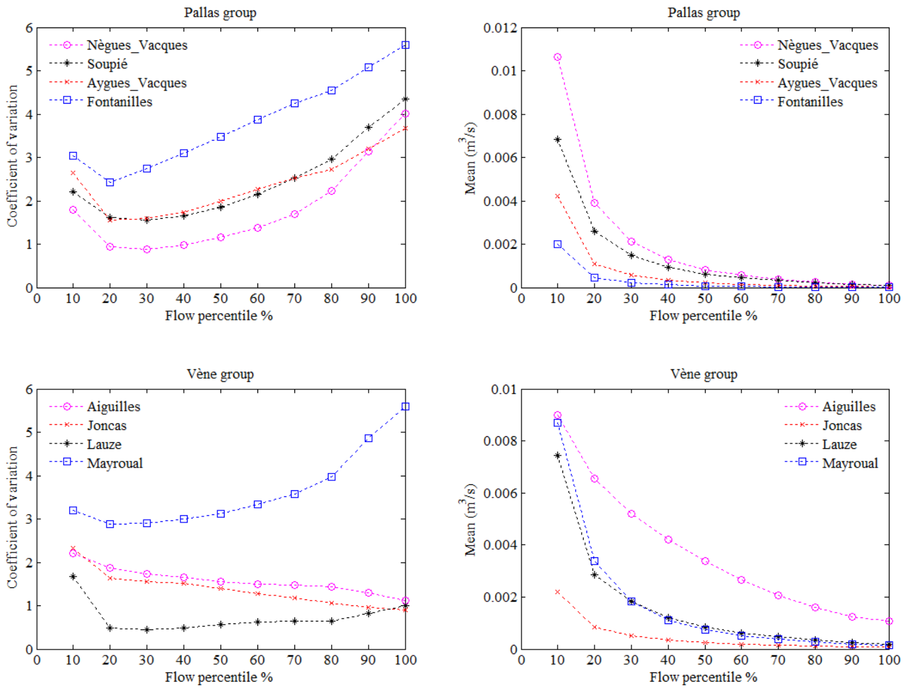

Fig. 6. Mean and coefficient of variation of the predicted FDCs percentiles based on the physical similarity approach for the Pallas catchments group (Pallas) and for the Vène catchments group (Vène).

HESSD
10, 4951–5011, 2013

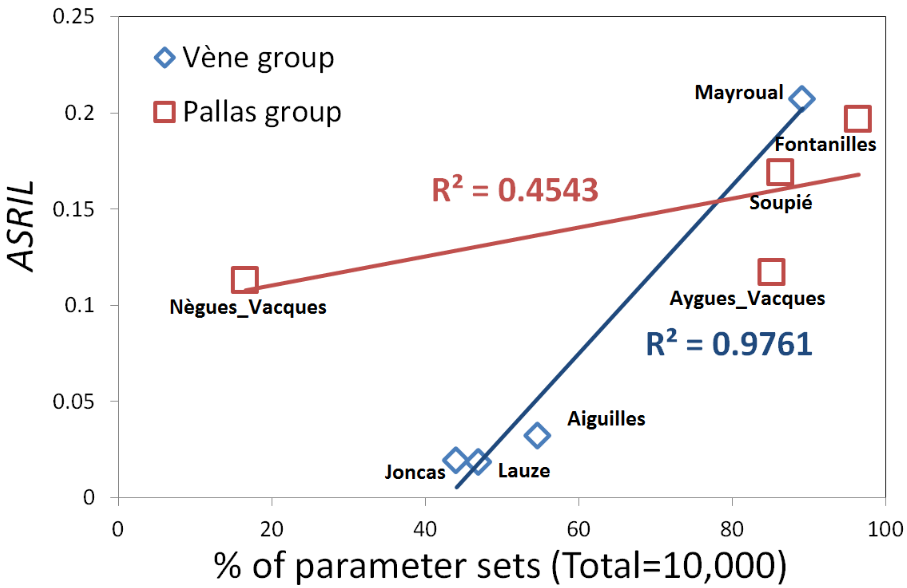

Fig. 7. Relationship between the number of transferred model parameter sets and the ASRIL factor at the ungauged catchments.

HESSD
10, 4951–5011, 2013

Uncertainty analysis in model parameters regionalization

H. Sellami et al.

Title Page
Abstract Introduction
Conclusions References
Tables Figures
◂◂ ▸▸
◂ ▸
Back Close
Full Screen / Esc
Printer-friendly Version
Interactive Discussion

HESSD
10, 4951–5011, 2013

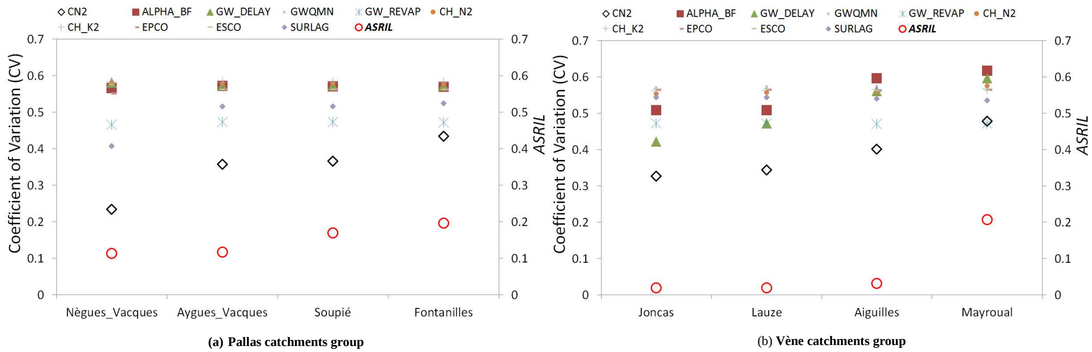

Fig. 8. Relationship between the CV variability of the transferred model parameter from gauged to the ungauged catchments and the ASRIL factor within each catchments group.

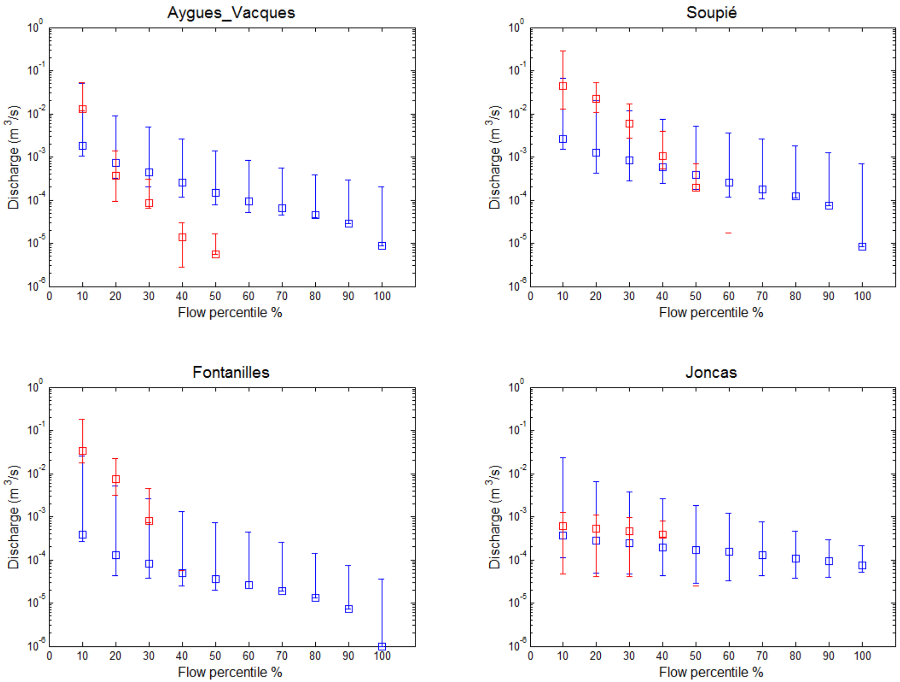

Fig. 9. 95 % uncertainty interval of the simulated FDCs flow percentiles versus 95 % of the observed FDCs flow percentiles resulting from the model parameters regionalization approach. Results correspond to the transfer of the Pallas model parameter sets to the Aygues_Vacques, Soupié and Fontanilles catchments and transfer of the Vène model parameters sets to the Joncas catchments. The blue color is for simulation and the red color is for observation. The bar corresponds to the 95 % flow percentile value while the square corresponds to the flow percentile median value.

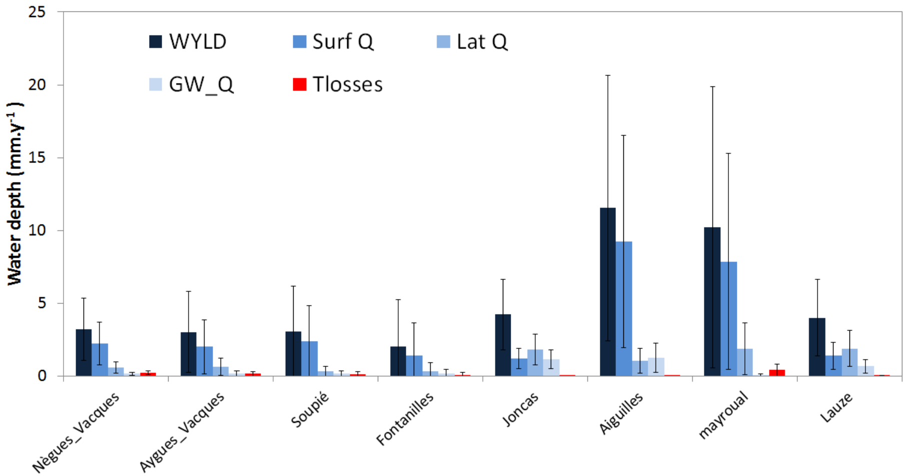

Fig. 10. Average annual water balance simulated at the ungauged catchments based on the regionalization approach. The error bars represent the standard deviation calculated based on all model simulations.

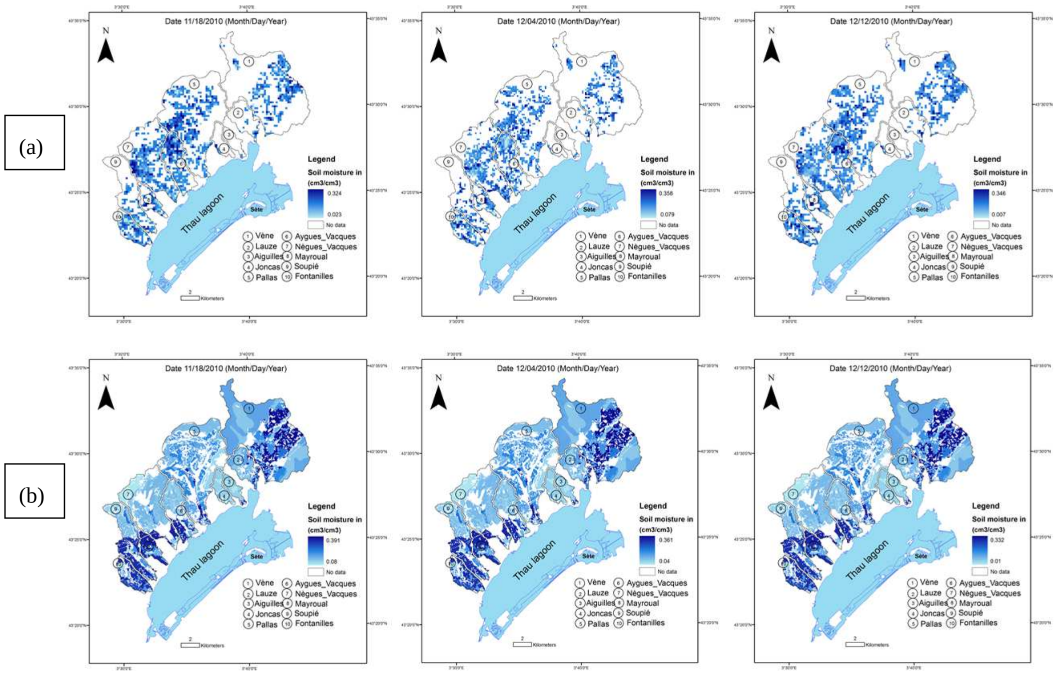

Fig. 11. Distribution of the soil moisture within the Thau catchment for 3 different dates; **(a)** is the "observed" soil moisture (Baghdadi et al., 2012) and **(b)** is the predicted soil moisture based on the regionalization results.

HESSD
10, 4951–5011, 2013

Uncertainty analysis in model parameters regionalization

H. Sellami et al.